



TECHNISCHE
UNIVERSITÄT
WIEN

Vienna University of Technology

D I P L O M A R B E I T

Emissions, deforestation and renewable resource harvesting under time-dependent environmental absorption efficiency

ausgeführt am Institut für
Stochastik und Wirtschaftsmathematik
der Technischen Universität Wien

unter der Anleitung von
Ao.Univ.Prof. Dipl.-Ing. Dr.techn. Gernot Tragler

durch

Andreas Steinwender

Steinergasse 13/2
1170 Wien

Wien, am 19. Mai 2015

(Unterschrift)

Eidesstattliche Erklärung

Hiermit erkläre ich, dass ich die vorliegende Arbeit selbständig verfasst und keine anderen als die angegebenen Quellen und Hilfsmittel benutzt habe und dass alle Stellen der Arbeit, die wörtlich oder sinngemäß aus anderen Quellen übernommen wurden, als solche kenntlich gemacht sind.

Wien, am 19. Mai 2015

(Unterschrift)

Abstract

In this Master's thesis, I describe an optimal control model about environmental pollution, where utility can be drawn from three different economic activities: production, deforestation and harvesting of a renewable natural resource. In this model the status of the environment is not only presented by the stock of pollution itself, but also by a so-called environmental absorption capacity, which describes the ability of the environment to absorb polluting emissions. It is investigated, under which conditions equilibrium points occur and which mix of the three different economic activities leads to an optimal equilibrium in the long run, considering their destructive impact on the environment. For that purpose, the numerical analyses are performed with the help of the MATLAB toolbox OCMat.

Keywords

optimal control theory / environmental pollution / environmental absorption efficiency / renewable natural resource / deforestation

Contents

1	Introduction	9
2	The Optimal Control Model	12
2.1	Model Formulation	12
2.2	Optimality Conditions	16
2.3	Steady State	17
3	Numerical Analysis	20
3.1	Base Case	21
3.1.1	Base parameters and OCMat initialization	21
3.1.2	Steady state	24
3.1.3	Time paths	31
3.2	Sensitivity Analysis	40
3.2.1	The discount rate r	40
3.2.2	Parameter a - Revenue from production	43
3.2.3	Parameter b - Revenue from deforestation	44
3.2.4	Parameter c - Revenue from harvesting	46
3.2.5	Parameter d - Costs of pollution	47
3.2.6	Parameter f - Carrying capacity of the renewable resource	48
3.2.7	Parameter α - Direct effect of deforestation on the pollution	49
3.2.8	Parameter γ - Influence of pollution on the absorption capacity	50
3.2.9	Summary	51
3.3	Other Parameter Scenarios	51
3.3.1	High discount rate r	52
3.3.2	Low discount rate r	55
3.3.3	Lower profits from deforestation	59
3.3.4	Lower costs of pollution	62
4	Summary and Conclusions	65

A Optimal Control Theory	67
B Overview of Results	69
List of Tables	70
List of Figures	71
Bibliography	72

Chapter 1

Introduction

In this Master's thesis, an optimal control model about environmental pollution is introduced, where utility can be drawn from three economic activities, i.e., production, deforestation and harvesting. Production and deforestation generate CO₂ emissions. Moreover, it is assumed that they have a negative influence on a renewable natural resource and therefore affect revenues from harvesting. Thus, the question is to find the optimal paths of these economic activities, which maximize revenue over an infinite horizon while also considering the social costs of pollution.

According to the latest report of the Global Carbon Project (Le Quéré et al. [2014]), CO₂ emissions from combustion of fossil fuel and cement production rose to 36 billion tons CO₂ in 2013, that is 61% above the emissions from 1990. Since 1750 atmospheric CO₂ concentration has increased by 43% and reached 395 parts per million on average in the year 2013, according to data from the US National Oceanic and Atmospheric Administration (Dlugokencky and Tans [2015]).

These increases of CO₂ emissions have crucial impact on the global climate. The Intergovernmental Panel on Climate Change (IPCC) has estimated global warming in the 21st century for different emission pathways. Results from the IPCC Fifth Assessment Report (IPCC [2013]) show that global surface temperature increase relative to the average from the years 1850 to 1900 is likely to exceed at least 1.5°C by 2100 in all their four sets of emission scenarios. The current trajectory of CO₂ emissions is tracking the baseline scenario with most emissions that suggests a temperature change between 3.2°C and 5.4°C.

There are already a number of models also considering the destructive impact of CO₂ emissions on the evolution of natural renewable resources. In the model presented in this thesis a formulation is suggested where this effect is considered indirectly by the environmental absorption efficiency. So the state of the environment is not only illustrated

by a stock of pollution, but also by the absorption efficiency rate.

This is motivated by Canadell et al. [2007], where they point out that a substantial part of the growth in atmospheric CO₂ is effected by a decrease of the absorption efficiency rate. Natural sinks on land and in oceans absorb part of the CO₂ emissions, so that the increase of the atmospheric CO₂ is smaller than the increase of anthropogenic CO₂ emissions. In Canadell et al. [2007] it is estimated that

“[...] 35 ±16% of the increase in atmospheric CO₂ growth rate between 1970–1999 and 2000–2006 was caused by the decrease in the efficiency of the land and ocean sinks in removing anthropogenic CO₂ (18 ±15%) and by the increase in carbon intensity of the global economy (17 ±6%). The remaining 65 ±16% was due to the increase in the global economy [...]”

In El Ouardighi et al. [2014] a pollution accumulation model is formulated with two state variables, the stock of pollution and the absorption capacity of the environment. These two state variables will also be considered in my model with similar transition equations. Whereas in El Ouardighi et al. [2014] the economy’s revenue is only determined by production, I formulate a model where the economy consists of three different economic activities by adding two control variables representing harvesting and deforestation.

An optimal control model investigating the link between harvesting of a renewable resource and pollution control is described in Tahvonen [1991], where it is assumed that the quality and the growth rate of the renewable resource is affected by the pollution stock. Similar to this paper, my model consists of a renewable resource, the dynamics of which are determined by the difference between a growth rate influenced by pollution and the amount of harvesting. However, while the negative externalities of pollution on the resource stock can be diminished only through reduced emissions in Tahvonen [1991], in my formulation the growth rate also depends on the environmental absorption capacity, which can be directly improved through an active effort of regeneration. This possibility can significantly alter the trade-off between the competing uses of the ecological environment, that is, the production of valuable natural resources or the use as a sink for polluting emissions.

The model in this Master’s thesis is taken from El Ouardighi [2015] and differs from the existing literature that assumes that the renewable resource stock is depleted by pollution flow linked either to consumption (Beltratti et al. [1994]) or to production (Ayong Le Kama [2001]). Instead of these direct influences of pollution on the resource, in my formulation there is an indirect influence through the environmental absorption efficiency, which determines the carrying capacity of the renewable resource stock.

This Master’s thesis is structured as follows. In Chapter 2 the optimal control model

will be introduced. Then necessary conditions for the steady state are set up by the use of Pontryagin's maximum principle. Since the canonical system cannot be solved analytically, a numerical approach is necessary. The results of the numerical analysis are presented in Chapter 3. The analysis is performed with the help of the MATLAB toolbox OCMat, and in this chapter also an introduction about using the OCMat toolbox is given. In Chapter 4 a summary of the results is given and conclusions are discussed, which can be drawn from the analysis.

Chapter 2

The Optimal Control Model

2.1 Model Formulation

I will reformulate a model described in detail in El Ouardighi [2015], where the social planner maximizes the economy's profit over an infinite horizon considering the environmental effects on future revenue.

As already mentioned in Chapter 1 the social planner can do this by dividing on the three economic sectors production, deforestation and harvesting of a renewable natural resource. These three economic activities are three of the four control variables in this model. The fourth decision variable determines the amount which is invested in restoration policies. These four controls influence the dynamics of the three state variables pollution stock, environmental absorption efficiency rate and renewable natural resource stock, which are described next.

As suggested by Canadell et al. [2007], CO₂ emissions are generated both by production and deforestation, while land and oceans are natural sinks that absorb part of these polluting emissions.

The emissions rate due to the production activity is denoted by $e(t) \geq 0$. The deforestation rate is denoted by $u(t) \geq 0$, and deforestation generates CO₂ emissions at a proportional rate $\alpha u(t)$, where $\alpha > 0$. While these two terms define the growth rate of the stock of pollution, it decreases at an environmental absorption efficiency rate $A(t)$. So the transition equation for the pollution stock is

$$\dot{P}(t) = e(t) + \alpha u(t) - A(t)P(t)$$

with the initial condition $P(0) = P_0 \geq 0$.

The dynamics of the environmental absorption efficiency rate $A(t)$ is given by the

equation

$$\dot{A}(t) = w(t) - u(t) - \gamma P(t)$$

with $\gamma > 0$ and the initial condition $A(0) = A_0 \geq 0$. Thus the environmental absorption efficiency rate decreases with the destructive impact of the stock of pollution and with deforestation. The parameter γ reflects the internal capacity of the environmental absorption efficiency to resist this destructive impact of pollution. On the other hand, the environmental absorption efficiency increases with a restoration effort, denoted by $w(t) \geq 0$. This assumption is motivated by the suggestion of Canadell et al. [2007], according to which reforestation policies can help increase the potential of biosequestration.

The dynamics of the pollution stock and the absorption efficiency are similar to those in El Ouardighi et al. [2014] with the extension of considering deforestation separately and the simplification that the government can control the development of the pollution stock only by the production rate without having a control variable representing a policy instrument to reduce emissions.

In El Ouardighi et al. [2014] the formulation and the dynamics of the pollution stock as well as the introduction of the environmental absorption efficiency are motivated in detail as described in what follows.

In the literature the transition equation for the pollution stock is most often of the form

$$\dot{P}(t) = e(t) - \kappa(P(t))$$

such that the pollution stock grows with rate of emissions $e(t)$ and is reduced by the effects of the environmental absorption capacity.

In lots of models a linear function is chosen as the characterization of the environmental absorption efficiency rate $\kappa(t)$. This makes the optimal control model more easy to solve, but this formulation doesn't fit well to the empirical observation that the environmental absorption capacity is depreciated when there is too much pollution. Moreover, part of land or sea reflecting the absorption capacity could even switch from a CO₂ sink to a CO₂ source.

A more realistic characterization is provided by a nonlinear absorption efficiency rate as used in some existing literature. However, those models are mathematically much more complex, which leads to limitations. To avoid those limitations, El Ouardighi et al. [2014] suggest to endogenize the absorption efficiency rate.

The third state variable is the stock of the renewable natural resource, denoted by $X(t) \geq 0$. Its development is described by the difference between the population growth rate $F(t) \geq 0$ and the harvesting rate $G(t) \geq 0$. So the dynamics of the renewable natural

resource are given by the differential equation

$$\dot{X}(t) = F(t) - G(t)$$

with a strict positive initial population stock $X(0) = X_0 > 0$.

As common for modelling population growth, I choose the logistic form for the growth rate of the resource stock:

$$F(t) = F(X(t), A(t)) = X(t) \left(1 - \frac{X(t)}{f(A(t))} \right),$$

where it is assumed that the carrying capacity $f(\cdot)$ depends positively on the environmental absorption rate, such that $f_A > 0$ and $f_{AA} \leq 0$. That means, the lower the environmental absorption rate, the lower the maximum stock of the renewable natural resource that the environment can sustain.

It follows from the logistic form that the growth rate $F(t)$ is zero when the population is zero (i.e., $F(X(t) = 0, A(t)) = 0$). Moreover, $F(t)$ is bounded from above, so that when there is no harvesting (i.e., $G(t) = 0$), the resource $X(t)$ converges to its maximal sustainable stock $f(A(t))$. For simplicity, I use a linear function such that $f(A(t)) = fA(t)$, where $f > 0$. With this specifications the environmental absorption rate has a concave increasing influence on the population growth, and $F(\cdot)$ satisfies the following properties:

$$F_A \geq 0, F_{AA} \leq 0, \left(F_X > 0 \Leftrightarrow X < \frac{fA}{2} \right), F_{XX} < 0, F_{XA} \geq 0 \text{ and } F_{XX}F_{AA} - (F_{XA})^2 = 0.$$

The harvesting rate $G(t)$ is given as multiplicative function of the harvesting effort $v(t) \geq 0$ and the renewable natural resource $X(t)$, such that

$$G(v(t), X(t)) = gv(t)X(t),$$

where $g > 0$ is the catchability coefficient.

Finally, I define the objective function for the social planner. The net utility function is assumed to be seperable additive in its arguments.

The economy's revenue function is supposed to be a concave increasing function of the emissions rate (reflecting the production rate), the deforestation rate and the natural renewable resource harvesting. For simplicity, I use logarithmic functions for all three economic activities, that is $a \ln e(t)$, $b \ln u(t)$ and $c \ln gv(t)X(t)$, where $a > 0$, $b > 0$ and $c > 0$.

The social costs generated by the destructive impact of the pollution stock are assumed

to be a convex increasing function, where I choose a quadratic function, that is $\frac{dP(t)^2}{2}$ with $d > 0$. For describing the costs of the policy instrument that aims at restoring and preserving the environmental absorption capacity, I also use a quadratic function, that is $\frac{kw(t)^2}{2}$. Without loss of generality, I can assume one of the multiplicative constants a, b, c, d , or k to be one. I will assume $k = 1$.

Furthermore, the parameter g and the control v only occur in the harvesting rate $G(t)$ as the product $gv(t)$. Thus, w.l.o.g., I can assume $g = 1$.

The aim of the social planner is to maximize the economy's net utility over an infinite planning horizon, where the discount rate is denoted by $r > 0$. So the optimal control problem is defined as follows:

$$\max_{e,u,v,w} \int_0^{\infty} e^{-rt} \left(a \ln e(t) + b \ln u(t) + c \ln (v(t)X(t)) - \frac{dP(t)^2}{2} - \frac{w(t)^2}{2} \right) dt \quad (2.1)$$

subject to

$$\dot{P}(t) = e(t) + \alpha u(t) - A(t)P(t) \quad (2.2)$$

$$\dot{A}(t) = w(t) - u(t) - \gamma P(t) \quad (2.3)$$

$$\dot{X}(t) = X(t) \left(1 - \frac{X(t)}{f(A(t))} - v(t) \right) \quad (2.4)$$

with initial conditions

$$P(0) = P_0 > 0, A(0) = A_0 > 0, \text{ and } X(0) = X_0 > 0, \quad (2.5)$$

subject to the control constraints

$$e(t) \geq 0, u(t) \geq 0, v(t) \geq 0, \text{ and } w(t) \geq 0 \quad (2.6)$$

and the state constraint

$$A(t) \geq 0 \quad (2.7)$$

for all t .

2.2 Optimality Conditions

The optimal control problem can be solved by using Pontryagin's maximum principle, which provides optimality conditions (see, e.g., Grass et al. [2008]). In Appendix A an overview about optimal control models and the maximum principle in general are given.

First, we need to derive the current-value Hamiltonian denoted by H . For convenience, the time argument t is omitted. Denoting the costate variables by $\lambda = (\lambda_1, \lambda_2, \lambda_3)$ the Hamiltonian for our model is of the following form:

$$H(P, A, X, e, u, v, w, \lambda) = a \ln e + b \ln u + c \ln(vX) - \frac{dP^2}{2} - \frac{w^2}{2} + \lambda_1(e + \alpha u - AP) + \lambda_2(w - u - \gamma P) + \lambda_3 X \left(1 - \frac{X}{fA} - v\right). \quad (2.8)$$

The dynamics of the costate variables $\lambda = (\lambda_1, \lambda_2, \lambda_3)$ follow from the maximum principle:

$$\dot{\lambda}_1 = r\lambda_1 - H_P = (r + A)\lambda_1 + \gamma\lambda_2 + dP, \quad (2.9)$$

$$\dot{\lambda}_2 = r\lambda_2 - H_A = r\lambda_2 + \lambda_1 P - \frac{\lambda_3 X^2}{fA^2}, \quad (2.10)$$

$$\dot{\lambda}_3 = r\lambda_3 - H_X = \lambda_3 \left(r - 1 + \frac{2X}{fA} + v\right) - \frac{c}{X}. \quad (2.11)$$

Next, according to the maximum principle the optimal control variables e^* , u^* , v^* and w^* maximize the Hamiltonian. Thus we have to solve

$$\max_{e, u, v, w} H(e, u, v, w)$$

and get the following necessary optimality conditions:

$$H_e = \frac{a}{e} + \lambda_1 = 0 \quad \Rightarrow \quad e = -\frac{a}{\lambda_1} \quad (2.12)$$

$$H_u = \frac{b}{u} + \alpha\lambda_1 - \lambda_2 = 0 \quad \Rightarrow \quad u = \frac{b}{\lambda_2 - \alpha\lambda_1} \quad (2.13)$$

$$H_v = \frac{c}{v} - \lambda_3 X = 0 \quad \Rightarrow \quad v = \frac{c}{\lambda_3 X} \quad (2.14)$$

$$H_w = -w + \lambda_2 = 0 \quad \Rightarrow \quad w = \lambda_2. \quad (2.15)$$

The Hessian matrix of the Hamiltonian w.r.t. the control variables,

$$\begin{pmatrix} H_{ee} & H_{eu} & H_{ev} & H_{ew} \\ H_{ue} & H_{uu} & H_{uv} & H_{uw} \\ H_{ve} & H_{vu} & H_{vv} & H_{vw} \\ H_{we} & H_{wu} & H_{wv} & H_{ww} \end{pmatrix} = \begin{pmatrix} -\frac{a}{e^2} & 0 & 0 & 0 \\ 0 & -\frac{b}{u^2} & 0 & 0 \\ 0 & 0 & -\frac{c}{v^2} & 0 \\ 0 & 0 & 0 & -1 \end{pmatrix}$$

is negative definite because of $a, b, c > 0$. Thus e^* , u^* , v^* and w^* given by

$$e^* = -\frac{a}{\lambda_1}, \quad (2.16)$$

$$u^* = \frac{b}{\lambda_2 - \alpha\lambda_1}, \quad (2.17)$$

$$v^* = \frac{c}{\lambda_3 X}, \quad (2.18)$$

$$w^* = \lambda_2, \quad (2.19)$$

maximize the Hamiltonian. By plugging the optimality conditions (2.16) - (2.19) into the canonical system (2.2) - (2.4) and (2.9) - (2.11)), we obtain the dynamics of the state variables and costate variables under optimal control:

$$\dot{P} = -\frac{a}{\lambda_1} + \frac{\alpha b}{\lambda_2 - \alpha\lambda_1} - AP, \quad (2.20)$$

$$\dot{A} = \lambda_2 - \frac{b}{\lambda_2 - \alpha\lambda_1} - \gamma P, \quad (2.21)$$

$$\dot{X} = X \left(1 - \frac{X}{fA} \right) - \frac{c}{\lambda_3}, \quad (2.22)$$

$$\dot{\lambda}_1 = (r + A)\lambda_1 + \gamma\lambda_2 + dP, \quad (2.23)$$

$$\dot{\lambda}_2 = r\lambda_2 + \lambda_1 P - \frac{\lambda_3 X^2}{fA^2}, \quad (2.24)$$

$$\dot{\lambda}_3 = \lambda_3 \left(r - 1 + \frac{2X}{fA} \right). \quad (2.25)$$

2.3 Steady State

Next we want to find the steady states of this optimal control model. For that purpose, we have to set the canonical system (2.20) - (2.25) equal to zero and have to solve the

following system of equations:

$$\begin{aligned}\dot{P} &= 0, \\ \dot{A} &= 0, \\ \dot{X} &= 0, \\ \dot{\lambda}_1 &= 0, \\ \dot{\lambda}_2 &= 0, \\ \dot{\lambda}_3 &= 0,\end{aligned}$$

which is equivalent to

$$-\frac{a}{\lambda_1} + \frac{\alpha b}{\lambda_2 - \alpha \lambda_1} - AP = 0 \quad (2.26a)$$

$$\lambda_2 - \frac{b}{\lambda_2 - \alpha \lambda_1} - \gamma P = 0 \quad (2.26b)$$

$$X \left(1 - \frac{X}{fA} \right) - \frac{c}{\lambda_3} = 0 \quad (2.26c)$$

$$(r + A)\lambda_1 + \gamma \lambda_2 + dP = 0 \quad (2.26d)$$

$$r\lambda_2 + \lambda_1 P - \frac{\lambda_3 X^2}{fA^2} = 0 \quad (2.26e)$$

$$\lambda_3 \left(r - 1 + \frac{2X}{fA} \right) = 0. \quad (2.26f)$$

This system of equations cannot be solved analytically completely. So we will need a numerical approach for deriving the steady states of this optimal control model.

Although the six-dimensional system (2.26) cannot be solved completely, it can at least be reduced to a lower-dimensional system. We start with deriving an expression for the state variable P by transforming Equation (2.26d) to

$$P = -\frac{1}{d} ((r + A)\lambda_1 + \gamma \lambda_2). \quad (2.27)$$

Besides some model parameters, the steady state of P in Equation (2.27) depends on the state variable A and also two costate variables.

From Equation (2.26c) we can get an expression for the costate variable λ_3 :

$$\lambda_3 = c \left(X \left(1 - \frac{X}{fA} \right) \right)^{-1}, \quad (2.28)$$

which is positive because of $c > 0$. As a consequence of $\lambda_3 > 0$, for satisfying Equa-

tion (2.26f) the term $r - 1 + \frac{2X}{fA}$ has to be equal to zero and thus we have

$$X = \frac{fA}{2}(1 - r). \quad (2.29)$$

Now we can plug the expressions for P , λ_3 and X from the Equations (2.27), (2.28) and (2.29) into the Equations (2.26a), (2.26b) and (2.26e):

$$-\frac{a}{\lambda_1} + \frac{\alpha b}{\lambda_2 - \alpha\lambda_1} + \frac{A}{d}((r + A)\lambda_1 + \gamma\lambda_2) = 0 \quad (2.30a)$$

$$\lambda_2 - \frac{b}{\lambda_2 - \alpha\lambda_1} + \frac{\gamma}{d}((r + A)\lambda_1 + \gamma\lambda_2) = 0 \quad (2.30b)$$

$$r\lambda_2 - \frac{\lambda_1}{d}((r + A)\lambda_1 + \gamma\lambda_2) - \frac{c}{A} = 0. \quad (2.30c)$$

So we have reduced the six-dimensional canonical system to the three-dimensional system (2.30).

Equation (2.29) shows that the steady state value of X only depends on the variable A besides the two model parameters f and r . As expected, the higher the carrying capacity fA , is the higher is the population X . Moreover, a lower discount rate r , which represents a more future-oriented behavior, leads to a higher long-run level of X .

If $r \geq 1$, the condition $X > 0$ is violated according to Equation (2.29). Therefore, for $r \geq 1$ no feasible steady state exists. We will observe the same result later during the numerical analysis.

Chapter 3

Numerical Analysis

For the numerical analysis I use the mathematical software MATLAB¹ together with the toolbox OCMat. OCMat is a MATLAB package designed for the analysis of optimal control models. Initiated by Dieter Grass around 2008, it has been developed continuously by Dieter Grass and colleagues such as Andrea Seidl from the research unit Operations Research and Control Systems (ORCOS), which is part of the Institute of Statistics and Mathematical Methods in Economics at TU Wien.

The numerical methods in the toolbox are based on the maximum principle with which the optimality conditions are derived. The optimal control model is formulated as a Boundary Value Problem (BVP) given by the canonical system. The BVP is analysed by using continuation methods varying the initial state, where an already calculated equilibrium point serves as trivial initial solution for the continuation. An introduction to optimal control models and the numerical methods used in the OCMat toolbox can be found in Grass et al. [2008].

A new version of the toolbox, OCMat2.0, was released in 2014 and can be downloaded for free at http://orcos.tuwien.ac.at/research/ocmat_software. In the following, I will not only present my results of the numerical analysis, but also explain how those results are derived with the help of the OCMat toolbox. So the reader will get a short introduction about how to use OCMat. For a detailed manual the reader is referred to Grass and Seidl [2014], while Grass [2012] exemplifies the numerical computation of the optimal vector field by a fishery model.

¹MATLAB is a registered trademark of The MathWorks, Inc.

3.1 Base Case

3.1.1 Base parameters and OCMat initialization

Before starting the analysis, the model parameter values have to be chosen. Since I couldn't find suggestions in the literature for setting the parameter values, I set the base parameters as given in Table 3.1 and provide an extensive sensitivity analysis, which is given in Section 3.2, in order to see the impacts of different parameter settings on the results.

Model parameter	Parameter value
r	0.4
a	1
b	1
c	1
d	2
f	10
α	0.5
γ	0.2

Table 3.1: Parameter settings for the base case

At the beginning of the analysis with OCMat some commands for the initialization of the model are necessary. First, an initialization file, providing all the specifications of the optimal control model, has to be written. The initialization file for the model analyzed in this thesis is named `emissions.ocm` and consists of the following lines:

Variable

independent

state::P,A,X

control::e,u,v,w

Statedynamics

ode::DP=e+alpha*u-A*P

ode::DA=w-u-gamma*P

ode::DX=X*(1-X/f/A)-v*X

Objective

expdisc::r

int::a*log(e)+b*log(u)+c*log(v*X)-d*P^2/2-w^2/2

Controlconstraint

CC1::ineq:e>=elb

CC2::ineq:u>=ulb

CC3::ineq:v>=vlb

CC4::ineq:w>=wlb

ArcDefinition

0::[]

1::CC1

2::CC2

3::CC3

4::CC4

5::CC1,CC2

6::CC1,CC3

7::CC1,CC4

8::CC2,CC3

9::CC2,CC4

10::CC3,CC4

11::CC1,CC2,CC3,CC4

Parameter

r::0.4

a::1

b::1

c::1

d::2

f::10

alpha::0.5

gamma::0.2

elb::0

ulb::0

vlb::0

wlb::0

The four sections `Variable`, `Statedynamics`, `Objective` and `Parameter` are mandatory in initialization files. Custom variable names can be chosen in the section `Variable`, which should improve the readability for the user. The dynamics of the model are specified in the section `Statedynamics`. In the Section `Objective` the discounted integral

that has to be maximized² is defined, where r denotes the discount rate. The parameter setting as given in Table 3.1 is carried out in Section `Parameter`.

In the lines following the signal word `Controlconstraint` the non-negativity conditions for the control are specified. In the section `ArcDefinition` arc-identifiers are assigned. The arc-identifiers indicate, which combination of control constraints are active or inactive. For example, in this model arc-identifier 5 would mean that the constraints `CC1` and `CC2` are active, while all others are inactive.

The next step is to process the initialization file. In this step the necessary optimality conditions are derived. This is done with the `OCMat` command

```
ocStruct=processinitfile('emissions');
```

Finally, some model files are generated and moved to the default model folder by calling the commands

```
m=stdocmodel('emissions');
modelfiles=makefile4ocmat(m);
moveocmatfiles(m,modelfiles);
```

Now all the preparation is done and we are ready to analyze the model.

Before starting the numerical analysis, we can use some useful `OCMat` commands getting model informations derived by `OCMat` in the initialization process. For example, with the command line

```
hamiltonian(m)
```

the symbolic expression of the Hamiltonian function is returned, which is the same as the Equation (2.8) derived in Section 2.2.

The canonical system (2.2) - (2.4) and (2.9) - (2.11) can be retrieved using `OCMat` by calling

```
canonicalsistem(m) .
```

The optimal control expressions that maximize the Hamiltonian (cf. Equations (2.16) - (2.18)) are returned by

```
control(m)
```

With the command

```
canonicalsistem(m, [], [], 1)
```

the control variables in the canonical system are substituted by their optimal expressions, and the expressions from the Equations (2.20) - (2.25) are returned.

²For a minimization problem, the objective function can be multiplied by minus one.

3.1.2 Steady state

We begin the numerical analysis with the search for equilibria of the canonical system. This can be done with the following OCMat commands:

```
ocEP=calcep(m);numel(ocEP)
b=isadmissible(ocEP,m,[],'UserAdmissible');ocEP(~b)=[];numel(ocEP)
ocEP{:}
[b_dim]=issaddle(ocEP{:})
store(m,ocEP);
```

which are explained in detail next.

The function `calcep` returns the equilibrium points of the optimal control model. For that purpose, it is first tried to solve the canonical system analytically by using the symbolic toolbox of MATLAB. For our model this fails. During the calculation, the message

```
Unable to find analytic solution. Resort to numerical method 'maple/fsolve'
```

is returned, and therefore MATLAB continues with a numerical calculation.

As retrieved by calling `numel(ocEP)`, 45 equilibria have been found and assigned to `ocEP`, which is an array of the solutions. However, not all of them have to be admissible equilibrium points. For instance, the first one

```
>> ocEP{1}
```

```
ans =
```

```
ocmatclass: dynprimitive
```

```
modelname: emissions
```

```
Equilibrium:
```

```
    0.7716
   -4.7080
  -14.1241
    0.3191
   -0.8431
   -0.1011
```


Eigenvalues:

6.5500
-6.1500
-0.5208
-0.2362
0.6362
0.9208

Arcidentifier:

0

has negative state variables, and the third one

>> ocEP{3}

ans =

ocmatclass: dynprimitive

modelname: emissions

Equilibrium:

-0.4163 + 0.4276i
-0.2107 - 0.5025i
-0.6321 - 1.5074i
1.8833 + 0.3298i
1.5523 + 0.1433i
-0.3380 + 0.8060i

Eigenvalues:

-1.0400 + 3.6254i
1.4400 - 3.6254i
-0.8616 + 0.0624i
-0.4359 - 0.0265i
1.2616 - 0.0624i
0.8359 + 0.0265i

Arcidentifier:

0

is a complex solution.

In order to check, which equilibria are admissible, the function `isadmissible` can be used. We can see that this model has only one admissible equilibrium:

```
>> b=isadmissible(ocEP,m,[],'UserAdmissible');ocEP(~b)=[];numel(ocEP)
ocEP{:}
```

```
ans =
```

1

```
ans =
```

```
ocmatclass: dynprimitive
```

```
modelname: emissions
```

Equilibrium:

0.7515

4.0056

12.0167

-0.3863

0.9932

0.1189

Eigenvalues:

-5.4454

5.8454

-0.5319

-0.2548

0.6548

0.9319

Arcidentifier:

0

Next the output

```
>> [b dim]=issaddle(ocEP{:})
```

b =

1

dim =

3

denotes that the equilibrium is a saddle point and that there are three negative eigenvalues, i.e., the corresponding stable manifold is three-dimensional. Finally, the equilibrium is stored to the model's results with the command

```
store(m,ocEP);
```

The arc-identifier zero of the OCMat output above denotes that all control constraints are inactive in the equilibrium point. By calling

```
>> control(m,ocEP{1})
```

ans =

2.5889

0.8429

0.7000

0.9932

the optimal values of the control variables in the equilibrium are returned. Similarly, the Hamiltonian is evaluated at the equilibrium point:

```
>> hamiltonian(m,ocEP{1})
```

```
ans =
```

```
1.8519
```

The results about the obtained steady state are summarized in Table 3.2. Considering the interpretation of the costate variables as shadow prices, i.e., the value of an additional infinitesimally small unit of the corresponding state variable, the signs of the costate variables are as expected: Pollution P has a negative effect, while the environmental absorption capacity A and the renewable natural resource X have a positive value.

It is interesting that the long-run production rate e^* is approximately three times higher than the deforestation rate u^* , although they have the same revenue function and the same coefficient in the objective function, $a = b = 1$. This allows for the interpretation that deforestation has a significantly more destructive impact on the environment by reducing the absorption efficiency and also increasing the stock of pollution.

State variables		Costate variables		Control variables	
P^*	0.75	λ_1^*	-0.39	e^*	2.59
A^*	4.01	λ_2^*	0.99	u^*	0.84
X^*	12.02	λ_3^*	0.12	v^*	0.70
				w^*	0.99

Table 3.2: Steady state values in the base case

Phase portrait

In order to better understand the behavior of the optimal control model, we have to create a phase portrait illustrating the stable manifold. For that purpose, we have to calculate the stable-paths from various initial points in order to get an idea how the steady state is approached from different initial conditions.

We begin with calculating a stable-path from the initial point $(P_0, A_0, X_0) = (0.05, 0.05, 0.05)$. This is done by calling the following OCMat commands:

```
opt=setoptions('OCCONTARG', 'MaxStepWidth', 2, 'MaxContinuationSteps', 250);
sol=initocmat_AE_EP(m,ocEP{1}, 1:3, [0, 0, 0], opt);
c=bvpcont('extremal2ep', sol, [], opt);
store(m, 'extremal2ep');
```

With `setoptions` some options for the continuation process can be adjusted. Further information for the available options can be found in Grass and Seidl [2014].

The continuation process is initiated with the function `initocmat_AE_EP`. The argument `ocEP{1}` specifies the equilibrium for which the stable-path is calculated and is also the initial solution for the boundary value problem (BVP). The third and the fourth argument denote the coordinates for which the continuation is processed and the corresponding values of the requested initial point.

Next the continuation process is executed by calling the command `bvpcont`, where the argument `'extremal2ep'` denotes a saddle-path continuation of an equilibrium point by varying the initial point. When the calculation is successful and the requested initial state is reached, the messages

```
Target value hit.  
label=HTV  
Continuation parameter=1
```

```
elapsed time = 57.9 secs
```

are displayed in the command window, and the calculated saddle-path can be stored to the model's result with the command

```
store(m,'extremal2ep');
```

Analogously the stable paths for nine more initial states are calculated: (0.05,0.05,20), (0.05,10,0.05), (0.05,10,20), (2,0.05,0.05), (2,0.05,20), (2,10,0.05), (2,10,20), (0.05,4,20) and (2,4,20). By calling

```
save(m)
```

all the model information and results are saved, which can later be retrieved with the following command lines:

```
m=stdocmodel('emissions');  
load(m)  
ocEP=equilibrium(m)  
ocAsym=extremalsolution(m)
```

Another useful function is the `delete`-function, which removes objects from the model's results. For example, the command

```
delete(m,'Continuation',[1, 2])
```

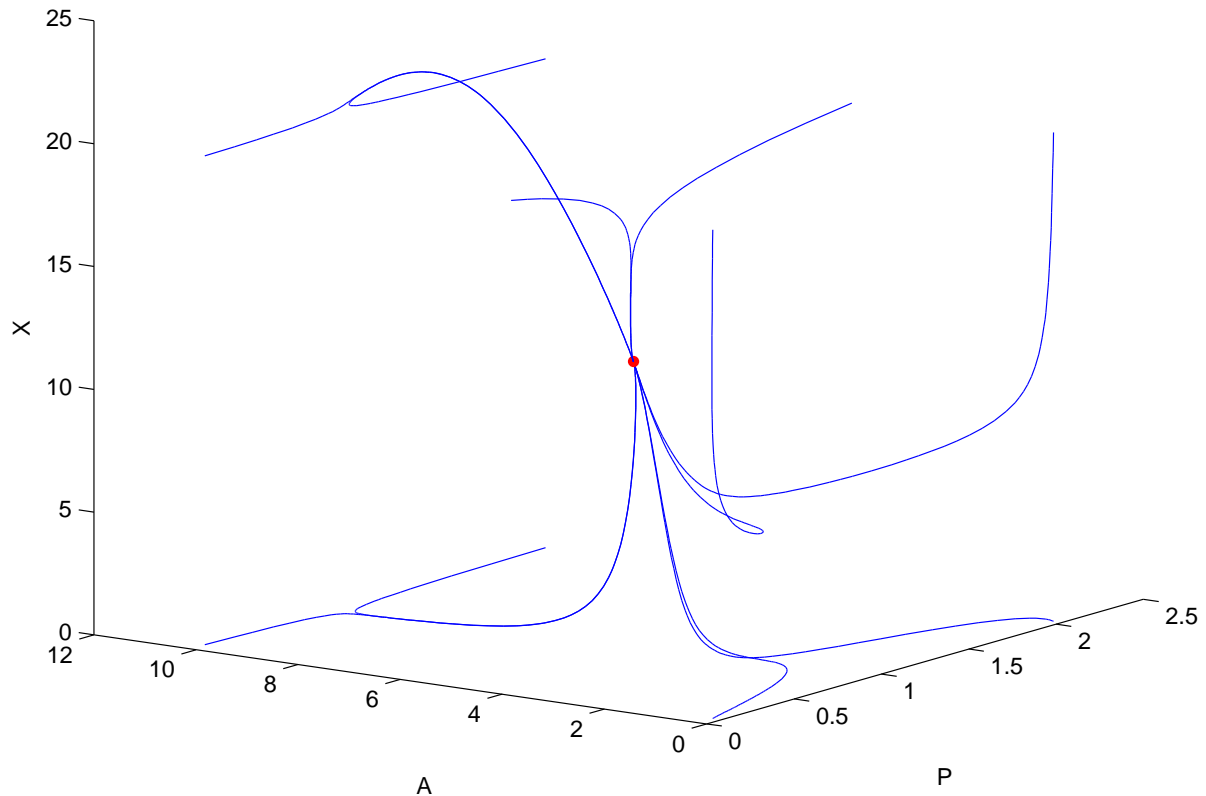


Figure 3.1: Phase portrait of the three state variables (pollution P , absorption capacity A , renewable natural resource X) for the base case.

removes the first two saddle-path continuations.

Now we can illustrate the calculated saddle-paths in a graphic. This could be done by using the standard MATLAB plotting commands. However, the OCMat toolbox also provides some helpful additional plotting functions.

A three-dimensional phase portrait of the state variables can be plotted by using the OCMat functions `plot3cont` and `plot3limitset`. Figure 3.1 is created with the following command lines:

```
clf
plot3cont(m,'state',1,'state',2,'state',3)
figure(gcf), view(3), hold on
plot3limitset(m,'state',1,'state',2,'state',3,'Marker','.', 'MarkerSize',15',
             'MarkerEdgeColor','r')
hold off
```

```

xlabel('P')
ylabel('A')
zlabel('X')
axis([0,2.5,0,12,0,25])
print('-r600','-depsc2','3dPhasePortrait.eps')
print('-r600','-djpeg','3dPhasePortrait.jpg')

```

In most starting positions the path to the steady state begins with first adjusting the level of the pollution stock P close to the equilibrium value, and only afterwards the levels of the environmental absorption capacity A and the renewable natural resource X begin to change towards the equilibrium level.

Only in the situation, where A is lower and X is higher than the steady-state values in the beginning, the pollution stock isn't changing that fast. These stable paths start with immediately decreasing the population of the resource X , initially even to lower levels than the equilibrium. Later the states A and P start to adjust.

On the other hand, in a situation with a high starting environmental absorption capacity A , it is optimal to first let the population of X increase, although it is already higher than the equilibrium population.

For the interpretation and further analysis of the dynamical system we will not only consider the state variables, but also the control variables. Since the optimal control model is quite complex and consisting of three states and four controls, interpreting phase portraits with combinations of states and controls would be rather confusing. Therefore we have to analyze time paths of the trajectories for some chosen initial states.

3.1.3 Time paths

For plotting the time paths, the OCMat function `plotcont`, the two-dimensional analogue to the function `plot3cont`, can be used. For example, by calling

```
plotcont(m,'time',1,'state',2,'index',[1],'Color','k','LineStyle','-')
```

the second state variable is plotted over time. With the arguments `'index',[1]` only the first trajectory is displayed in this plot. Most of the standard MATLAB plotting properties can also be used for the function `plotcont`.

All the plots in this subsection are created with the following command lines, where i is the number of the trajectory that should be plotted:

```

clf
subplot(7,1,1), plotcont(m,'time',1,'control',1,'index',[i],'Color','k')
axis([0,20,0.6,2.8])

```

```

xlabel('t')
ylabel('e')
box on
subplot(7,1,2), plotcont(m,'time',1,'control',2,'index',[i],'Color','k')
axis([0,20,0.4,1])
xlabel('t')
ylabel('u')
box on
subplot(7,1,3), plotcont(m,'time',1,'control',3,'index',[i],'Color','k')
axis([0,20,0.4,0.8])
xlabel('t')
ylabel('v')
box on
subplot(7,1,4), plotcont(m,'time',1,'control',4,'index',[i],'Color','k')
axis([0,20,0.9,2])
xlabel('t')
ylabel('w')
box on
subplot(7,1,5), plotcont(m,'time',1,'state',1,'index',[i],'Color','k',
'LineStyle','-.')
xlabel('t')
ylabel('P')
axis([0,20,0,1])
box on
subplot(7,1,6), plotcont(m,'time',1,'state',2,'index',[i],'Color','k',
'LineStyle','-.')
xlabel('t')
ylabel('A')
axis([0,20,0,4])
box on
subplot(7,1,7), plotcont(m,'time',1,'state',3,'index',[i],'Color','k',
'LineStyle','-.')
xlabel('t')
ylabel('X')
axis([0,20,0,15])
box on
set(gcf,'PaperPosition',[0.25,2.5,8,12])

```



```
print('-r600', '-depsc2', strcat('Trj', num2str(i), '_TimePath.eps'))
print('-r600', '-djpeg', strcat('Trj', num2str(i), '_TimePath.jpg'))
```

We start with analyzing the time paths for the trajectory with initial states $(0.05, 0.05, 0.05)$, which are displayed in Figure 3.2. In this situation, there is almost no pollution P in the beginning, but on the other hand the environmental absorption efficiency A and the stock of the renewable natural resource X are also nearly zero.

Although there is so little pollution in the beginning, the production level starts with $e \approx 1$, i.e., there are much lower emissions than in the steady state. Similarly the deforestation rate u is lower and the restoration effort w is higher in the starting situation than in steady state. That is mainly because initially there is almost no support from the environmental absorption capacity reducing the growth rate of pollution. So P increases extremely fast, and at $t \approx 1.5$ the stock of pollution is already a little bit higher than its equilibrium level. The three above mentioned controls e , u and w remain stable for a short period before they almost simultaneously start to change significantly towards their equilibrium values. Because of the initial path of the controls, the state A can grow pretty fast. At $t \approx 2$, the environmental absorption efficiency has already reached half of its steady-state level. But soon the slope diminishes because of the changes of e , u and w . Moreover, the pollution is already that high that it has a significant destructive impact on the absorption capacity. The renewable natural resource X remains almost zero in the beginning because of the low carrying capacity. Not before A has already reached a high level, the population X can grow significantly. While the dynamics of the three controls e , u , w are rather interconnected, the harvesting rate v seems to depend mainly on the development of the corresponding resource X . In the initial state, the control v is also lower than its steady-state value. It starts growing rather slowly and later a little bit faster, when X is beginning to rise.

The second trajectory has the initial states $(0.05, 0.05, 20)$. Thus the only difference to the starting situation analyzed above is that the initial population of the renewable natural resource X isn't almost zero; here it is almost twice the equilibrium level.

In the beginning, X falls immediately down to almost 5, before it recovers at $t \approx 2$ and begins growing towards the equilibrium level, as we can observe in the time paths in Figure 3.3. That is because in the beginning the population of X is much higher than the carrying capacity fA .³ Moreover, the harvesting rate v is initially also pretty high. The explanation for this high initial harvesting rate could be that it is economically better to take profit of this high resource stock instead of waiting until the population would naturally reach its carrying capacity. And it seems that the environmental absorption

³So this starting situation is a quite unnatural situation.

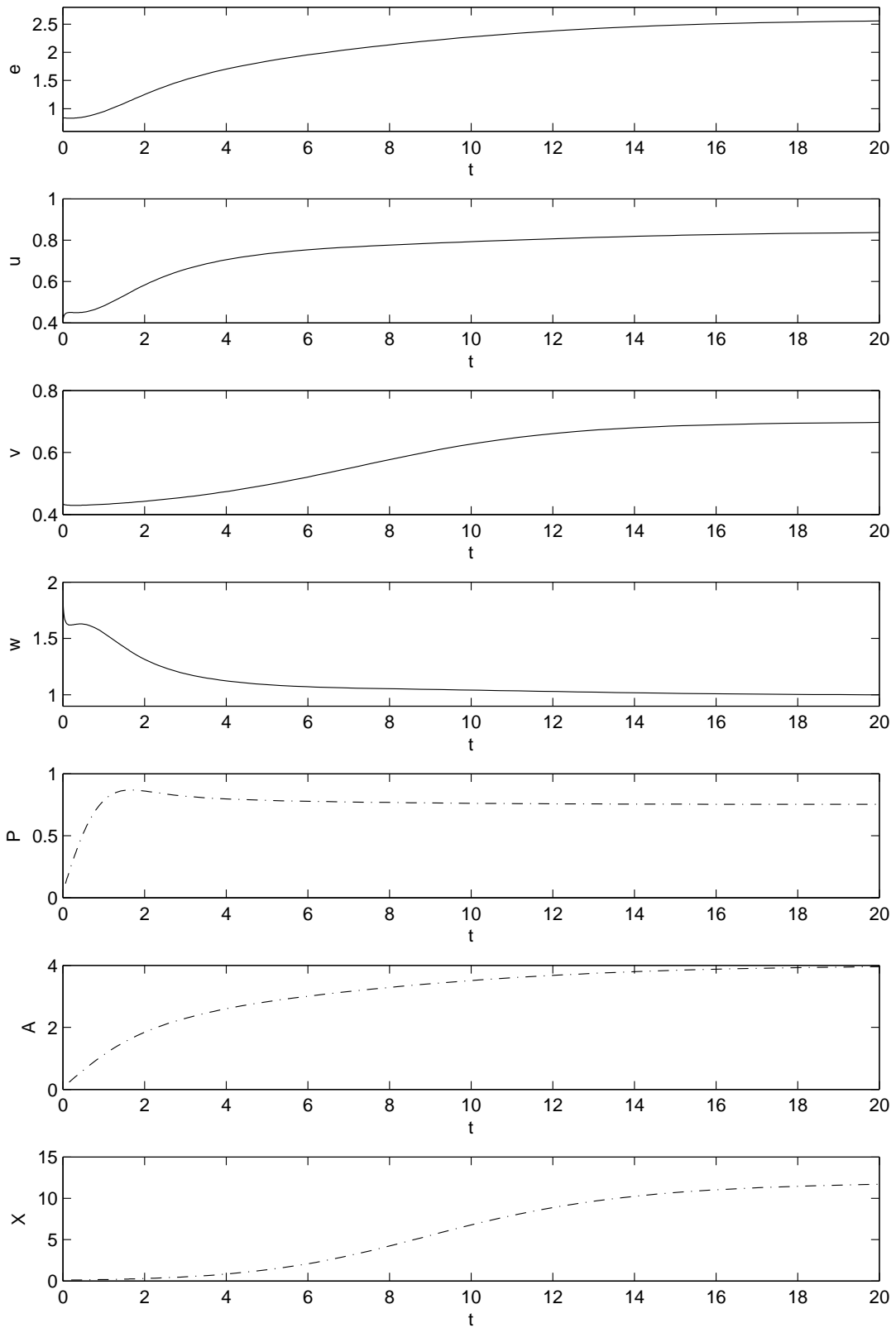


Figure 3.2: Time paths of the four control variables (production e , deforestation u , harvesting v , restoration w) and the three state variables (pollution P , absorption capacity A , renewable natural resource X) for the trajectory starting in $(0.05, 0.05, 0.05)$.

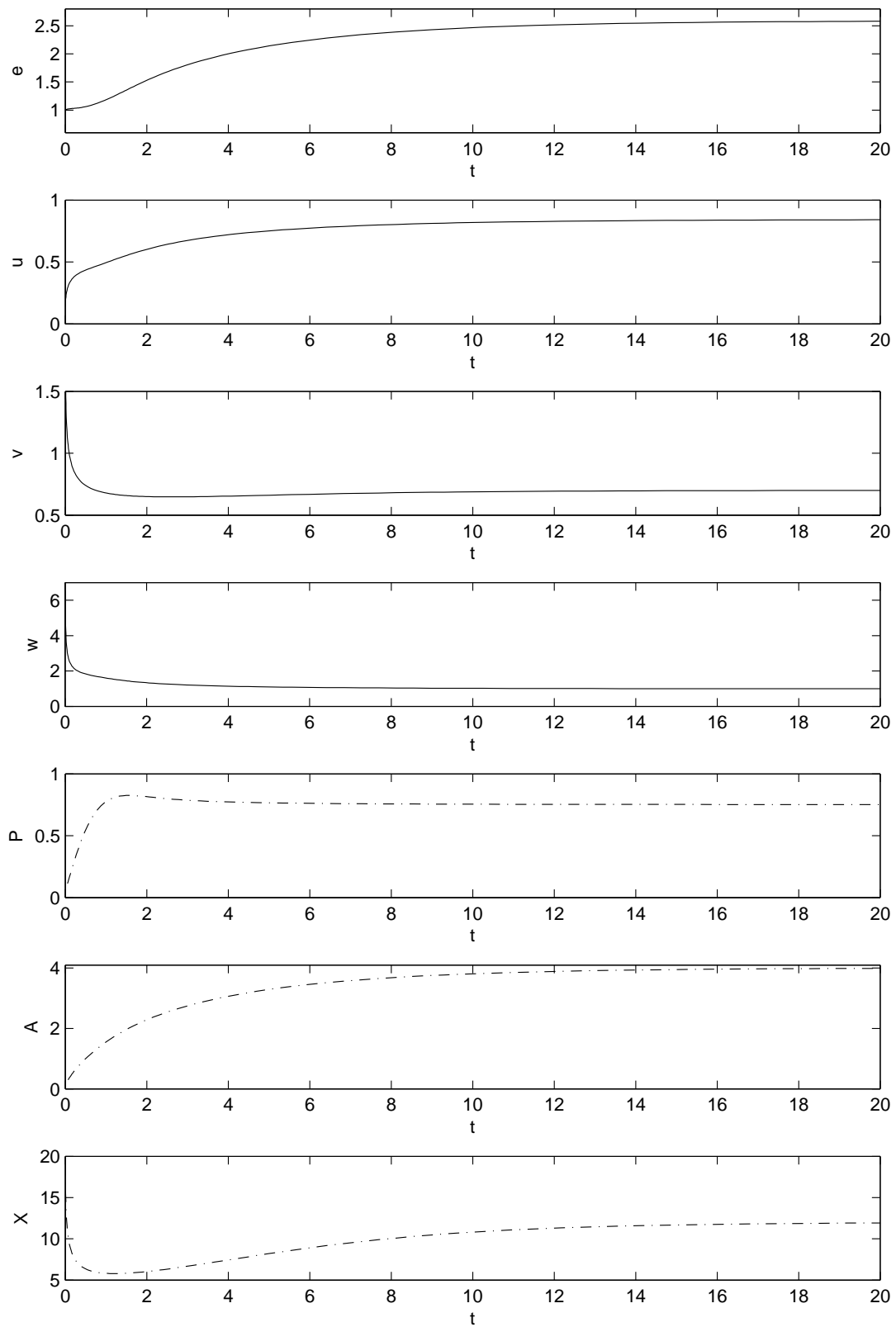


Figure 3.3: Time paths of the four control variables (production e , deforestation u , harvesting v , restoration w) and the three state variables (pollution P , absorption capacity A , renewable natural resource X) for the trajectory starting in $(0.05, 0.05, 20)$.

capacity A and so the carrying capacity can't grow fast enough to preserve the population of the resource X on a level that high. The restoration effort w in the beginning is even more than five times higher than in the equilibrium, but still the slope of A isn't extremely steep. The dynamics of the production e and pollution P are basically the same as for the first trajectory. So the pollution stock reaches the steady-state level almost as soon as for other initial situations. This wasn't clear from just looking at the phase portrait in Figure 3.1 because X is changing so quickly in this situation.

In Figure 3.4, the time paths for the trajectory starting in the state $(0.05, 10, 0.05)$ are displayed. The dynamics of the state X and the control v are the same as in Figure 3.2. It doesn't seem to make a difference that A has a higher initial value in this case, since in the other starting scenario driven by the growing A the carrying capacity increases fast enough. However, the development of the pollution stock P is different. Although for the two trajectories analyzed so far, the pollution stocks reach the equilibrium level very soon, in this situation the slope of P is even higher in the beginning. That is because here it is no problem when the environmental absorption capacity A decreases, since A is much higher than in the steady state. Thus production e and the deforestation rate u are very high in the beginning, while the restoration effort starts with $w \approx 0.5$ lower than in the equilibrium value.

The most favorable initial conditions are when the pollution P is low and when the absorption efficiency A and the population of the renewable natural resource X are initially high. Figure 3.5 shows the time paths for such a trajectory starting in the initial states $(0.05, 10, 20)$.

The only different time paths compared with Figure 3.4 are the ones for the control v and the state X . It seems that a different initial value of X mostly only has an influence on the dynamics of itself and on the harvesting rate v . With the population of X starting at 20, far above the equilibrium level, it nevertheless increases a little bit in the beginning before decreasing towards 12. The harvesting rate v starts already near its steady-state value and doesn't change a lot on the way to the equilibrium.

In contrast to the situation described above, the most adverse initial conditions considered here are when there are almost no environmental absorption capacity and renewable natural resource but a high pollution stock in the beginning. The time paths for such a scenario are displayed in Figure 3.6, where the trajectory has the initial states $(2, 0.05, 0.05)$.

Again the time paths for X and v are the same as we have already seen with other trajectories. Compared to the first trajectory we investigated, starting in $(0.05, 0.05, 0.05)$ and displayed in Figure 3.2, the time paths for the other three controls e , u and w vary a

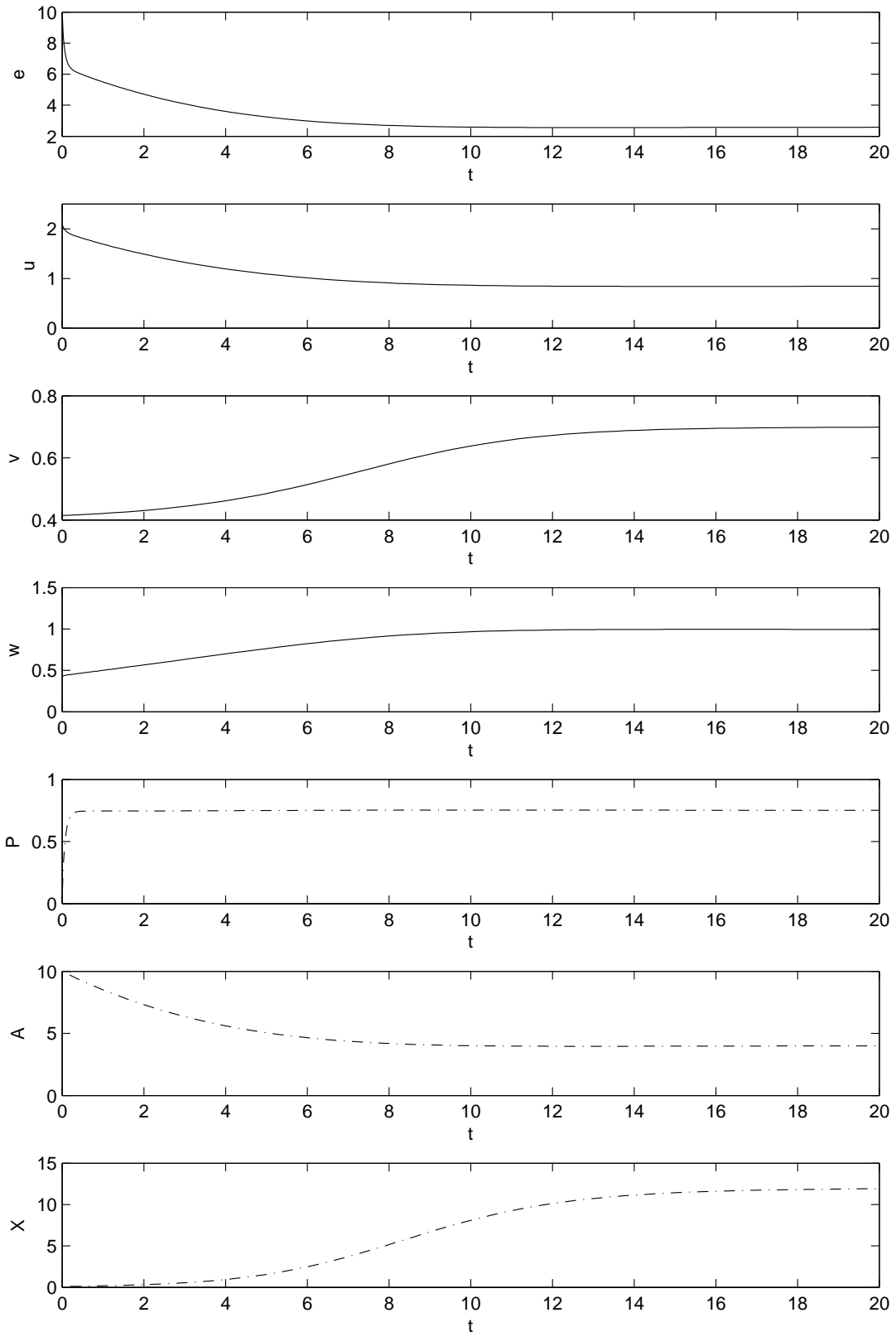


Figure 3.4: Time paths of the four control variables (production e , deforestation u , harvesting v , restoration w) and the three state variables (pollution P , absorption capacity A , renewable natural resource X) for the trajectory starting in $(0.05, 10, 0.05)$.

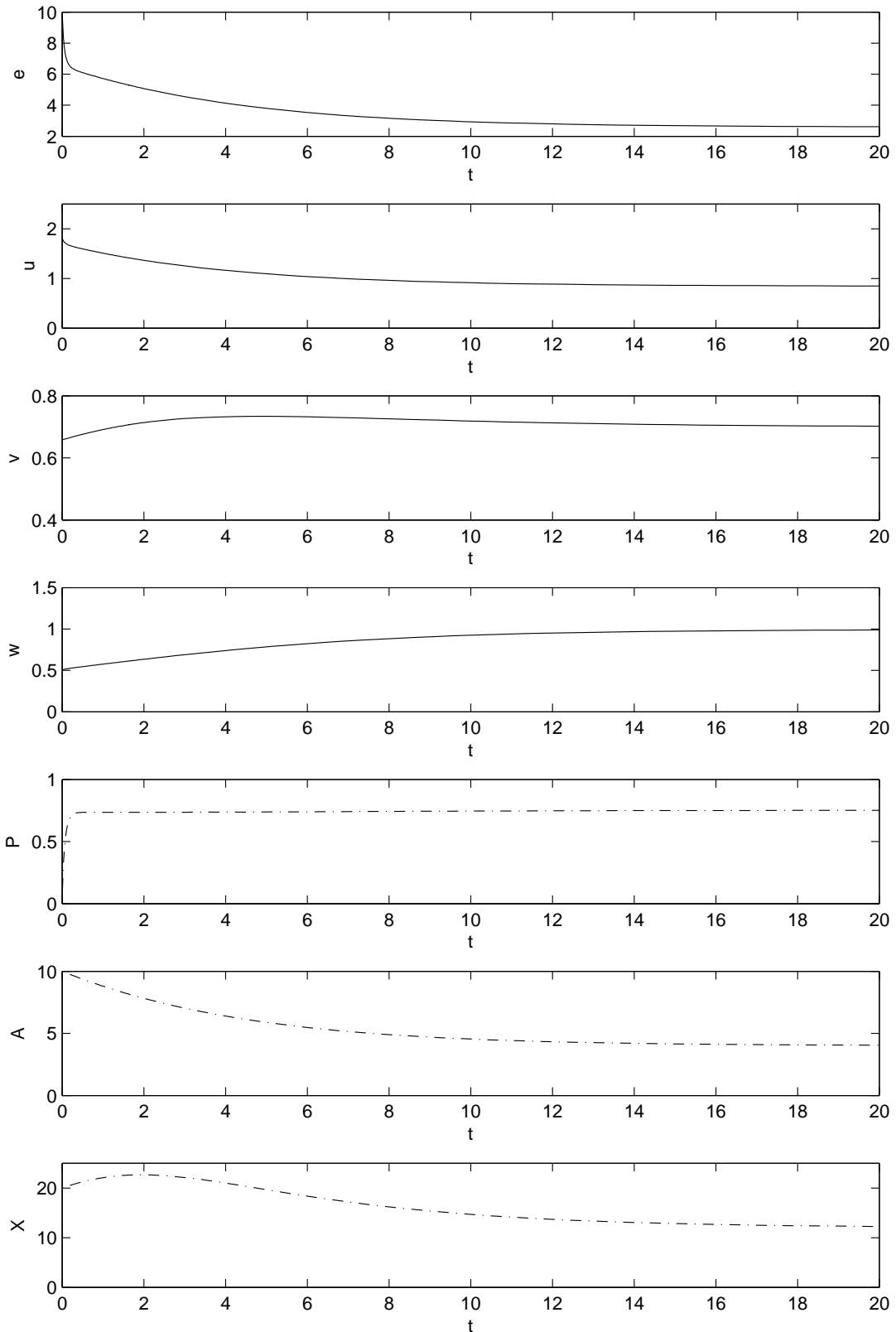


Figure 3.5: Time paths of the four control variables (production e , deforestation u , harvesting v , restoration w) and the three state variables (pollution P , absorption capacity A , renewable natural resource X) for the trajectory starting in $(0.05, 10, 20)$.

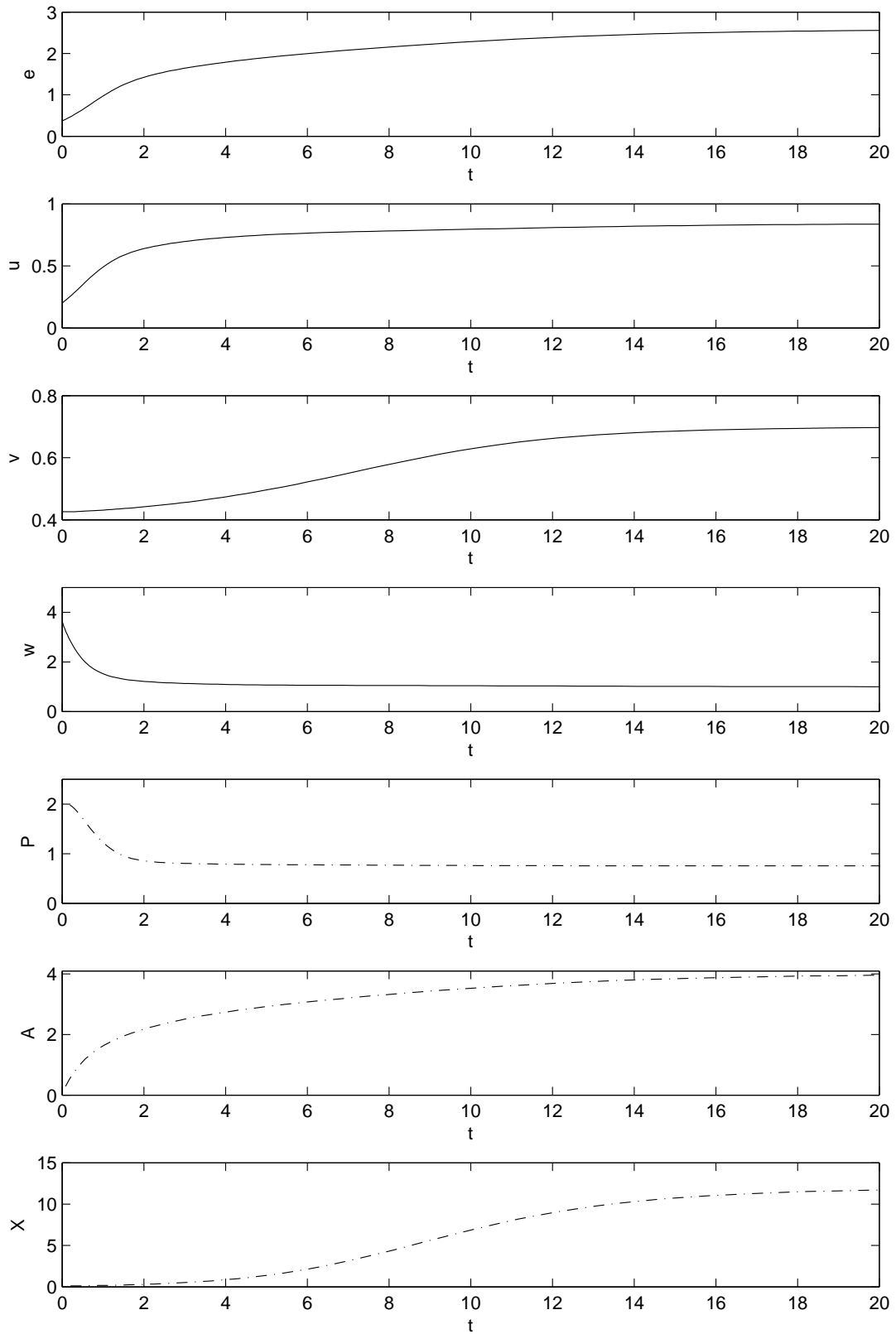


Figure 3.6: Time paths of the four control variables (production e , deforestation u , harvesting v , restoration w) and the three state variables (pollution P , absorption capacity A , renewable natural resource X) for the trajectory starting in $(2, 0.05, 0.05)$.

little bit right in the beginning, but soon they are quite similar. Since the pollution stock X is high and the absorption capacity A is almost zero, initially the restoration effort w is much higher, and also the production e and u are starting at low levels. However, together with the support of a fast rising absorption capacity, at $t = 2$ the pollution stock has already decreased to $P \approx 1$, not much higher than in the steady state.

3.2 Sensitivity Analysis

As already mentioned in the beginning of Subsection 3.1.1, we need to perform a sensitivity analysis. Since we don't have reliable studies about the parameter values, we have to investigate the effects of changing parameter values on the equilibrium and whether bifurcations and scenarios with multiple equilibria occur or not.

The continuations required for creating bifurcation diagrams can be processed with the MATLAB toolbox MatCont. Additionally, the OCMat toolbox offers some functions that are useful for employing OCMat together with MatCont. The OCMat function `contep` continues a equilibrium by using the MatCont toolbox. For further information about the MatCont toolbox the reader is referred to Dhooge et al. [2006].

The continuation of the equilibrium by varying the parameter r is done by calling the following command lines:

```
opt=setoptions('MATCONT','MaxStepsize',5e-2,'MaxNumPoints',5000,
'Backward',0);
[X1, V1, S1]=contep(m,ocEP{1},parameter,opt);
opt=setoptions(opt,'MATCONT','MaxStepsize',5e-2,'MaxNumPoints',5000,
'Backward',1);
[X2, V2, S2]=contep(m,ocEP{1},parameter,opt);
S1.msg
S2.msg
```

The equilibrium has to be continued twice to change the parameter in both directions. The direction of the continuation process is set by the option `'Backward'`. The `contep`-outputs `S1.msg` and `S2.msg` return information about occurring special points.

Now the results and interpretations from the continuation of all model parameters are presented.

3.2.1 The discount rate r

We start the sensitivity analysis by investigating the behavior of the steady state when the discount rate r is varied between zero and one. In the base case, r is set 0.4.

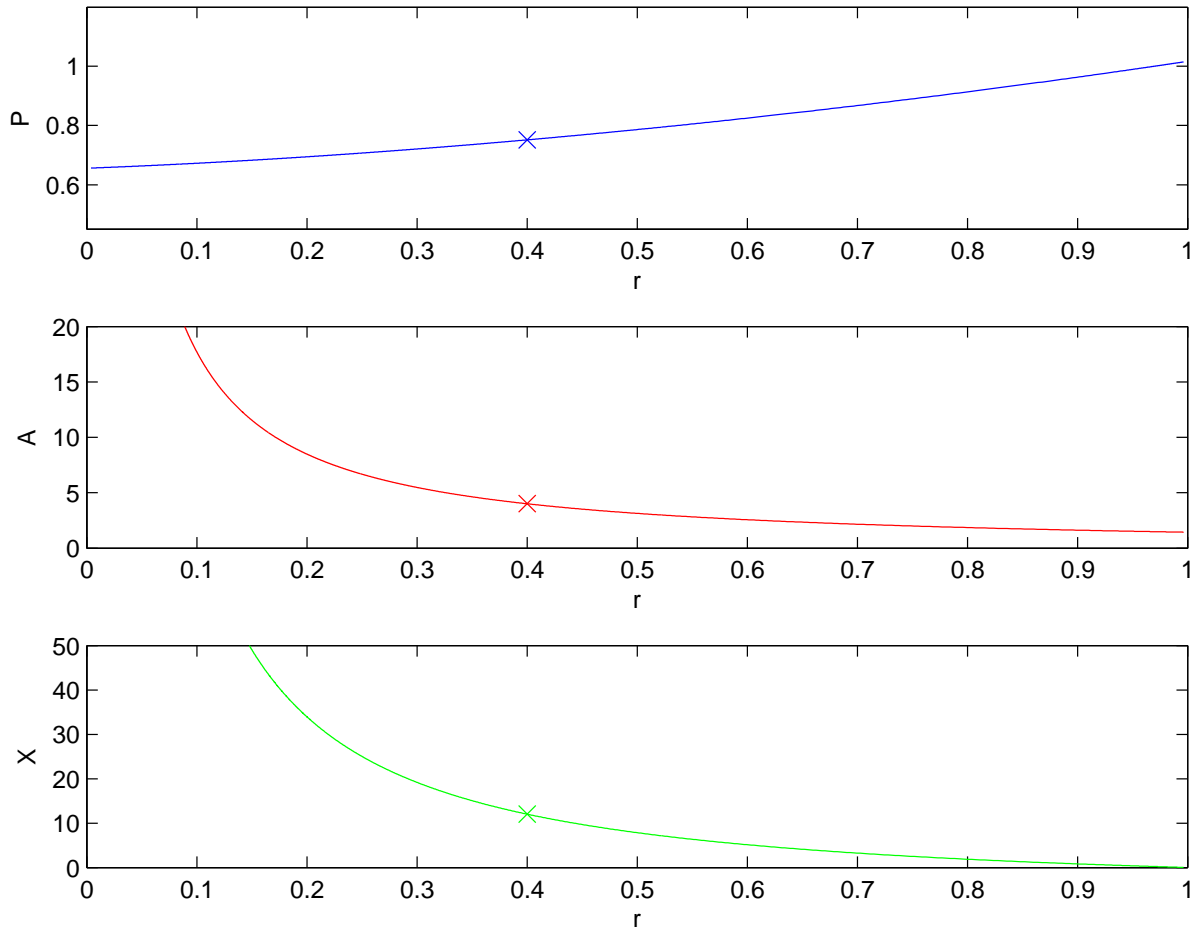


Figure 3.7: Bifurcation diagram for the parameter r : The upper panel displays the steady-state values for the pollution stock P , the middle one for the environmental absorption efficiency A and the lower one for the renewable natural resource X .

The discount rate determines how future benefits or costs are exponentially discounted. A low discount rate means that people (in this model the social planner) are far-sighted and future benefits aren't much less worth than present benefits. In the contrary, a high discount rate means that they are present-oriented, i.e., benefits in the far future are significantly less worth compared to present benefits.

Figure 3.7 displays the bifurcation diagram for the discount rate r , and there is another figure (3.8) showing the equilibrium values of A and X for small values of r .

In the first panel of Figure 3.7, we can see that the discount rate r has a positive effect on the stock of pollution P , which isn't really surprising: When the people are myopic, they mostly care about present benefits and exploit the environment accepting the pollution to increase and therefore having lower benefits in the long run.

With the same interpretation, the optimal value of the absorption capacity A decreases

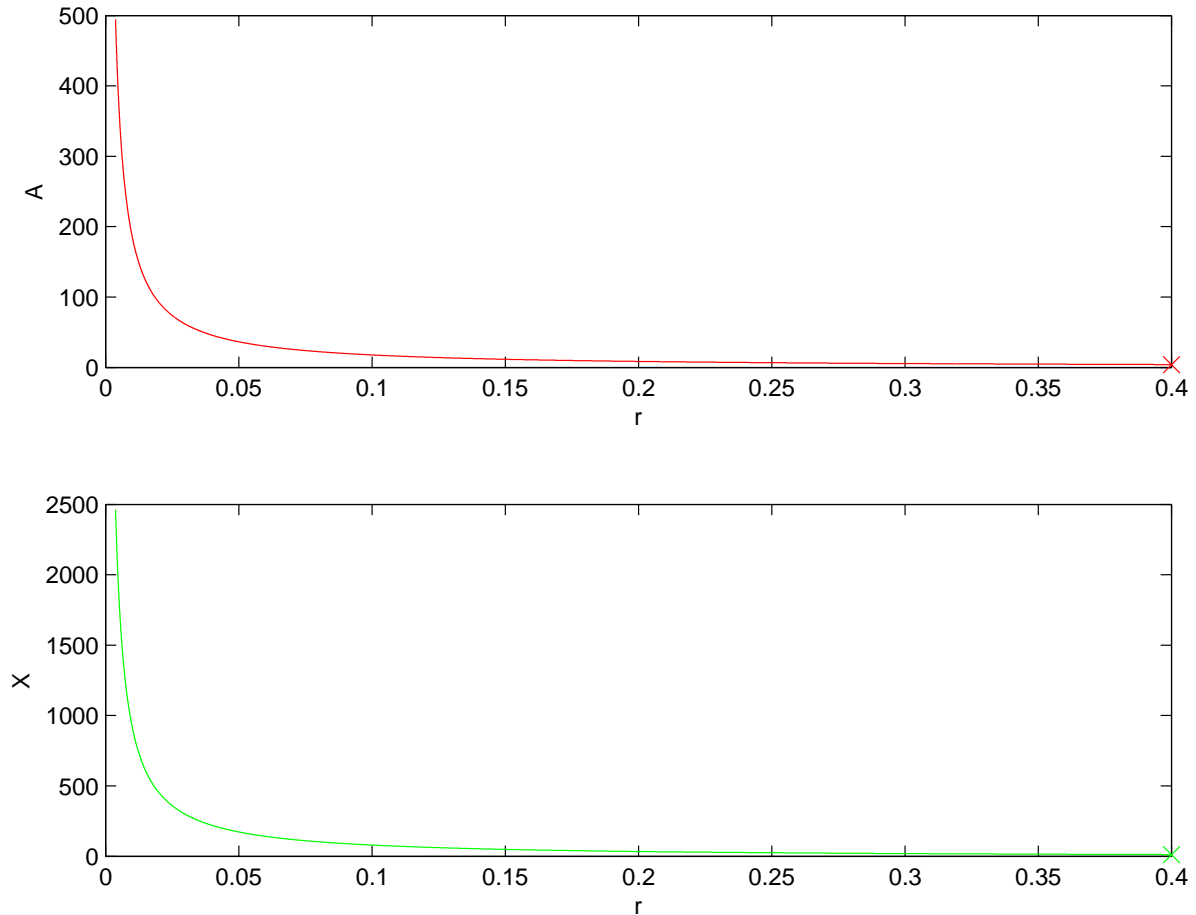


Figure 3.8: Bifurcation diagram for small r : The upper panel displays the steady-state values for the pollution stock P , the middle one for the environmental absorption efficiency A and the lower one for the renewable natural resource X .

with rising r . However, while the steady state of the pollution isn't reduced much for a smaller value of r , the optimal absorption capacity is getting extremely high when r is very small, as we can see in more detail in Figure 3.8.

The shape of the bifurcation curve of the renewable natural resource X is similar to the one for A , but even a little bit more extreme. For r going to one, the steady-state population of X is converging to zero. If the social planner is future-oriented, it is optimal to let X grow to a high level in order to have sustainable benefits from harvesting in the future. But when the social planner is very myopic, s/he prefers to have more benefits in the present even accepting that the resource is going to extinct.

As already shown in the end of Section 2.3, for r greater or equal to one, no feasible equilibrium point exists.

3.2.2 Parameter a - Revenue from production

The profit function for the production e is a logarithmic function with the multiplicative constant a : $a \ln e$. Figure 3.9 shows the optimal steady-state values for a varying between zero and three. The base case value for a is one.

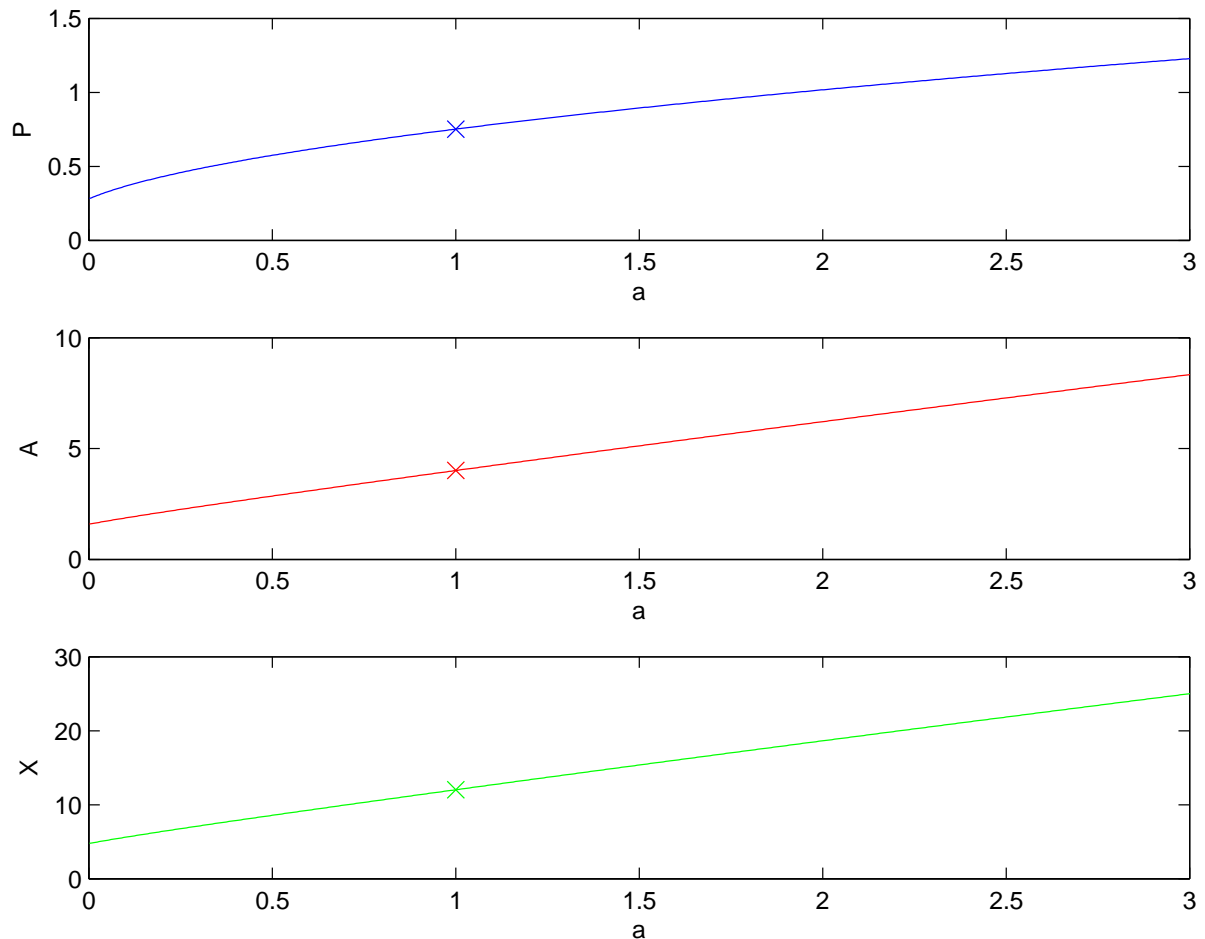


Figure 3.9: Bifurcation diagram for the parameter a : The upper panel displays the steady-state values for the pollution stock P , the middle one for the environmental absorption efficiency A and the lower one for the renewable natural resource X .

With a higher value for the parameter a , there is more revenue from production and therefore the equilibrium level of pollution P is higher. For $a = 3$ the optimal long-run value of P is already greater than 1.2.

The effect of varying the parameter a doesn't only concern the production, it also makes the other economical activities, deforestation and harvesting, less attractive compared to production.⁴ Therefore, in a situation where a is higher, the deforestation rate

⁴In the base case, the three multiplicative parameters a , b and c have the same value.

decreases a little bit. That is a reasonable explanation for the relatively higher equilibrium level of A . And with a higher value of A , the carrying capacity of the renewable natural resource X is higher and thus X is able to reach a higher sustainable level.

3.2.3 Parameter b - Revenue from deforestation

Next we consider the profit function for the deforestation, which is a logarithmic function with the multiplicative constant b : $b \ln u$. Figure 3.10 shows the optimal steady-state values for b varying between zero and three. The base case value for b is one.

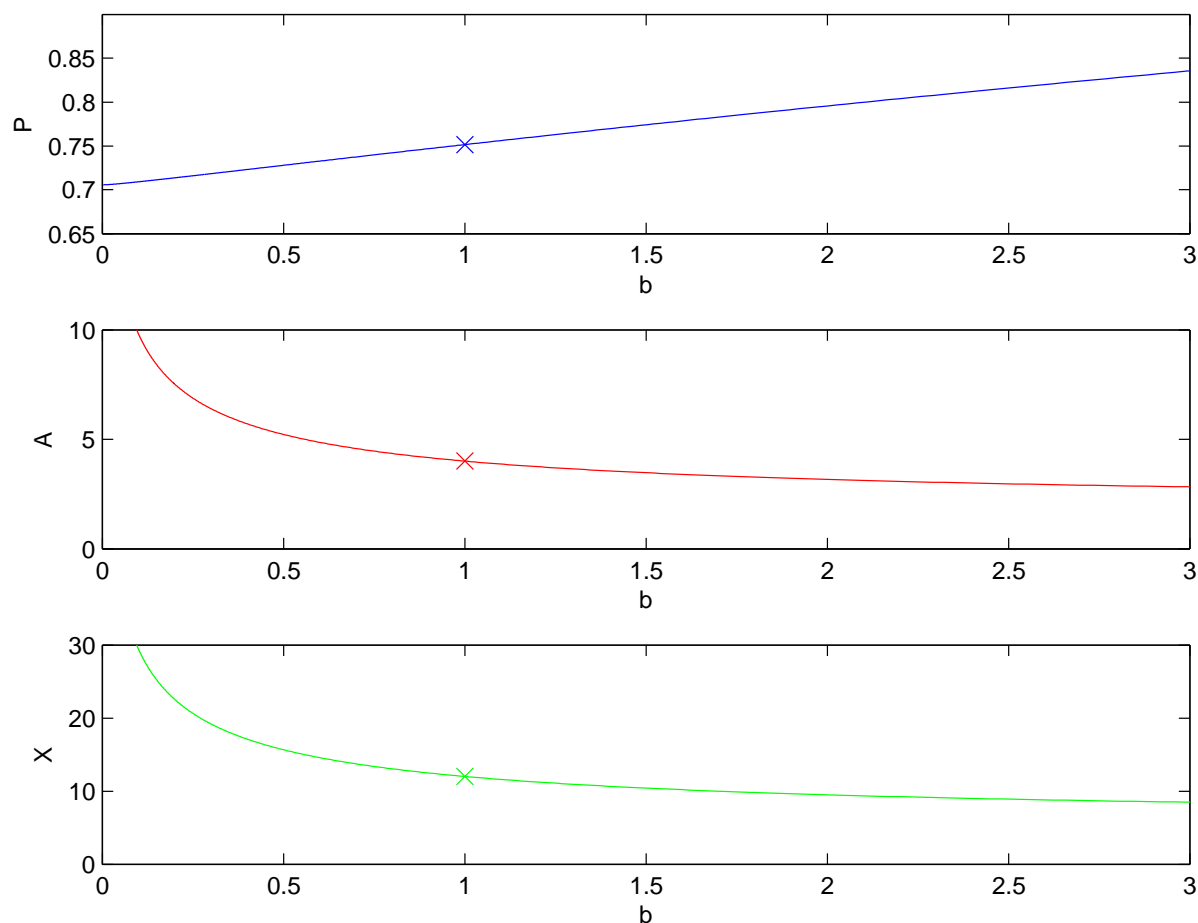


Figure 3.10: Bifurcation diagram for the parameter b : The upper panel displays the steady-state values for the pollution stock P , the middle one for the environmental absorption efficiency A and the lower one for the renewable natural resource X .

With b rising, the optimal steady state of A decreases, since deforestation gets more attractive. A little surprising is that the optimal stock of pollution P is also slightly higher, although the production rate decreases as expected.⁵ However, the negative im-

⁵For $b = 3$ the optimal long-run production rate e^* is approximately 1.6, compared to 2.6 in the base

pact of deforestation on the pollution is twofold: First, it directly increases the production growth rate and second, the growth rate rises indirectly through the decrease in the absorption capacity A . Thus the positive influence of lower production rate is outweighed by those effects. Again the equilibrium value of the resource X seems to mainly depend on the one for A .

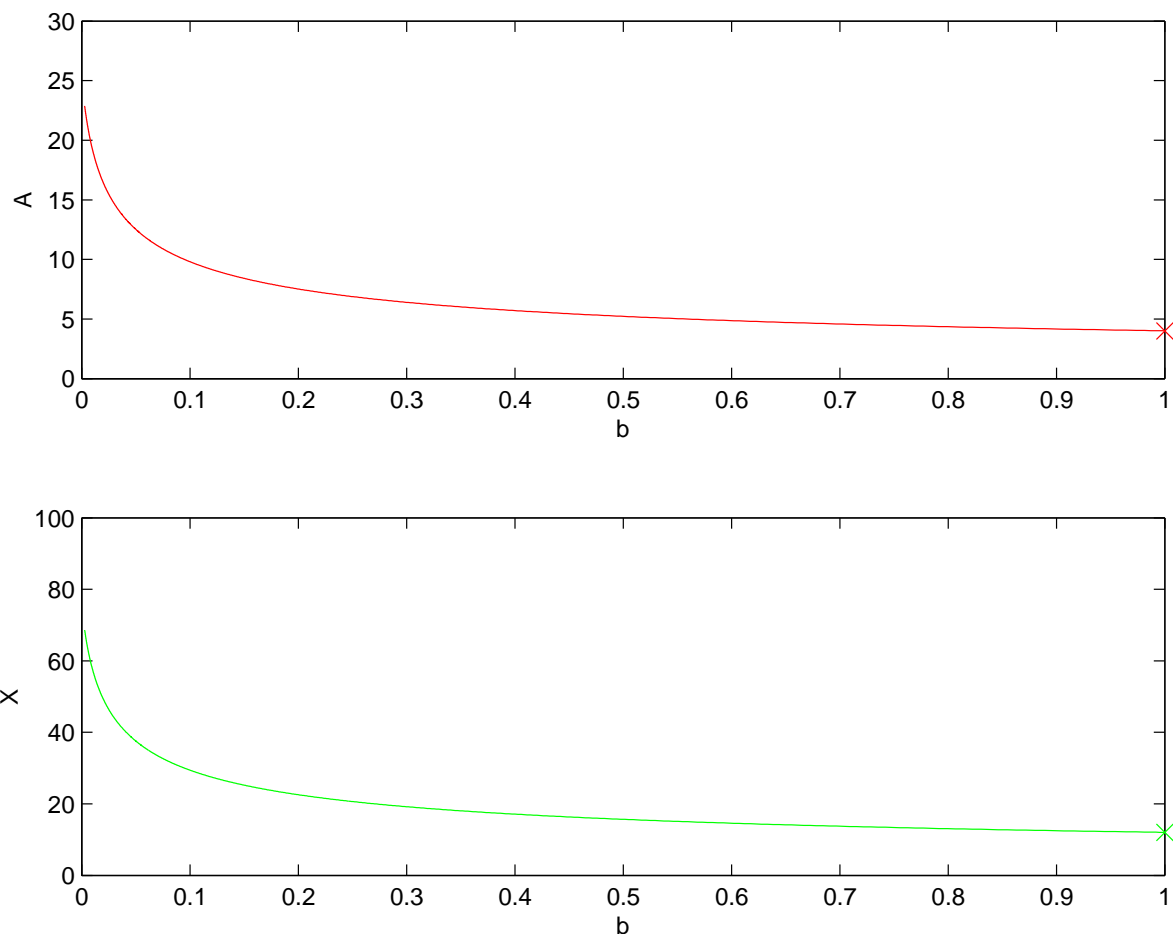


Figure 3.11: Bifurcation diagram for small b : The upper panel displays the steady-state values for the pollution stock P , the middle one for the environmental absorption efficiency A and the lower one for the renewable natural resource X .

It is also particularly interesting that a small value of the parameter b and consequently a low optimal deforestation rate has an extremely positive effect on the equilibrium level of the environmental absorption efficiency A (see Figure 3.11).

case where $b = 1$.

3.2.4 Parameter c - Revenue from harvesting

The last economic activity is harvesting of a renewable natural resource. The corresponding parameter of the logarithmic revenue function ($c \ln vX$) is the multiplicative constant c . In Figure 3.12 the bifurcation diagrams for c varying between zero and three are displayed. The base case value for c is one.

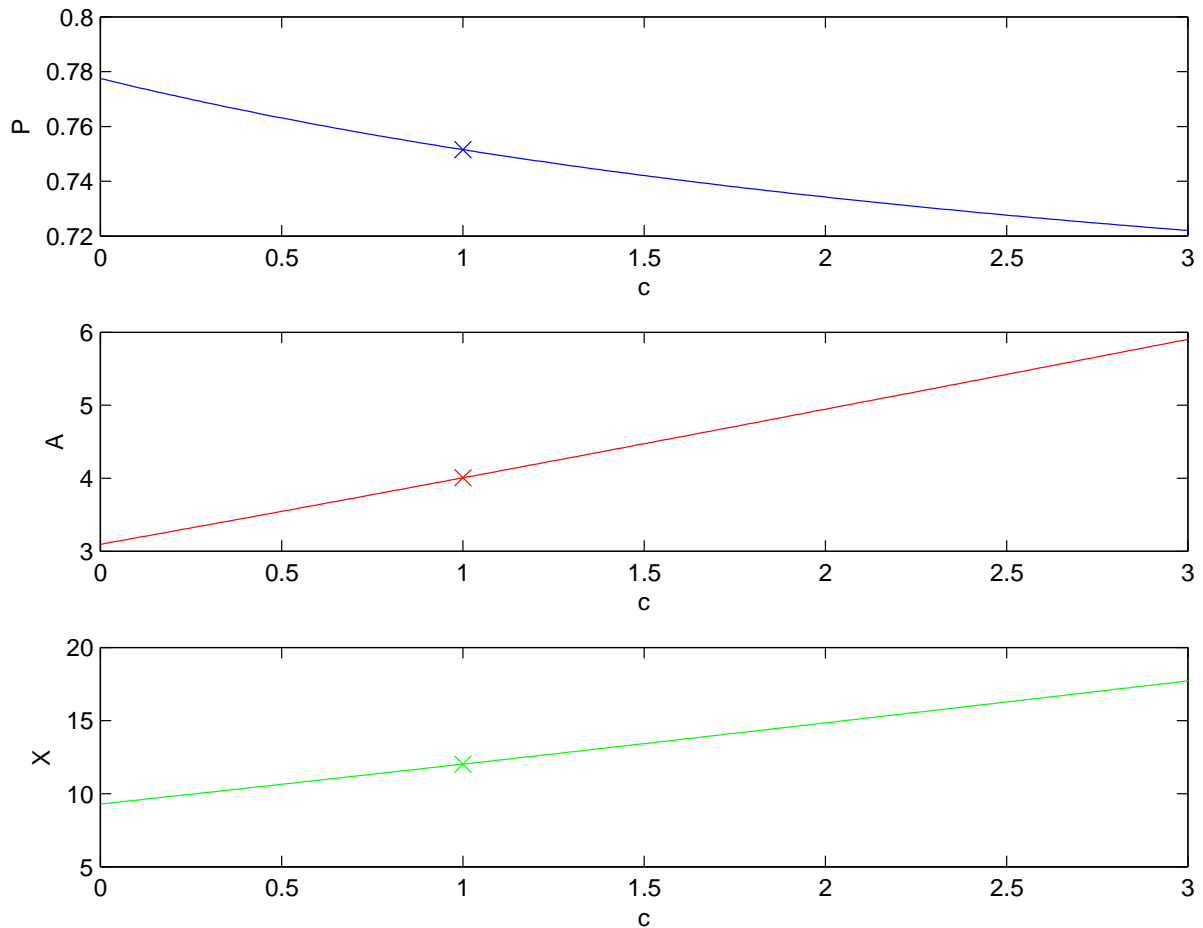


Figure 3.12: Bifurcation diagram for the parameter c : The upper panel displays the steady-state values for the pollution stock P , the middle one for the environmental absorption efficiency A and the lower one for the renewable natural resource X .

The interpretation of this bifurcation diagram is analogous to the one for the parameters a and b . A higher weight for revenues from harvesting makes the other two economic activities, production and deforestation, less attractive. Therefore, with increasing c the optimal steady-state value of the absorption capacity A increases while the one of pollution P decreases. We can also see that the equilibrium levels don't change that much with varying c compared to other parameters.

3.2.5 Parameter d - Costs of pollution

The cost function measuring the negative effects of pollution is a quadratic function with multiplicative parameter d : $\frac{dP^2}{2}$. The base value of d is two. The bifurcation diagrams for d between 0 and 10 can be seen in Figure 3.13.

For d increasing from the base value two the effect on the equilibrium levels of the state variables is quite little, but for d getting close to zero the slope of the bifurcation curves changes significantly. Again the direction of the changes are not surprising. A low value of d means that pollution isn't evaluated that bad, and thus the optimal steady-state value of P is higher. But the pollution also has a negative impact on the environmental absorption capacity A and so the steady state of A and X is lower. While the impact of varying d on P is quite significant compared to other parameters, A and X don't change that much.

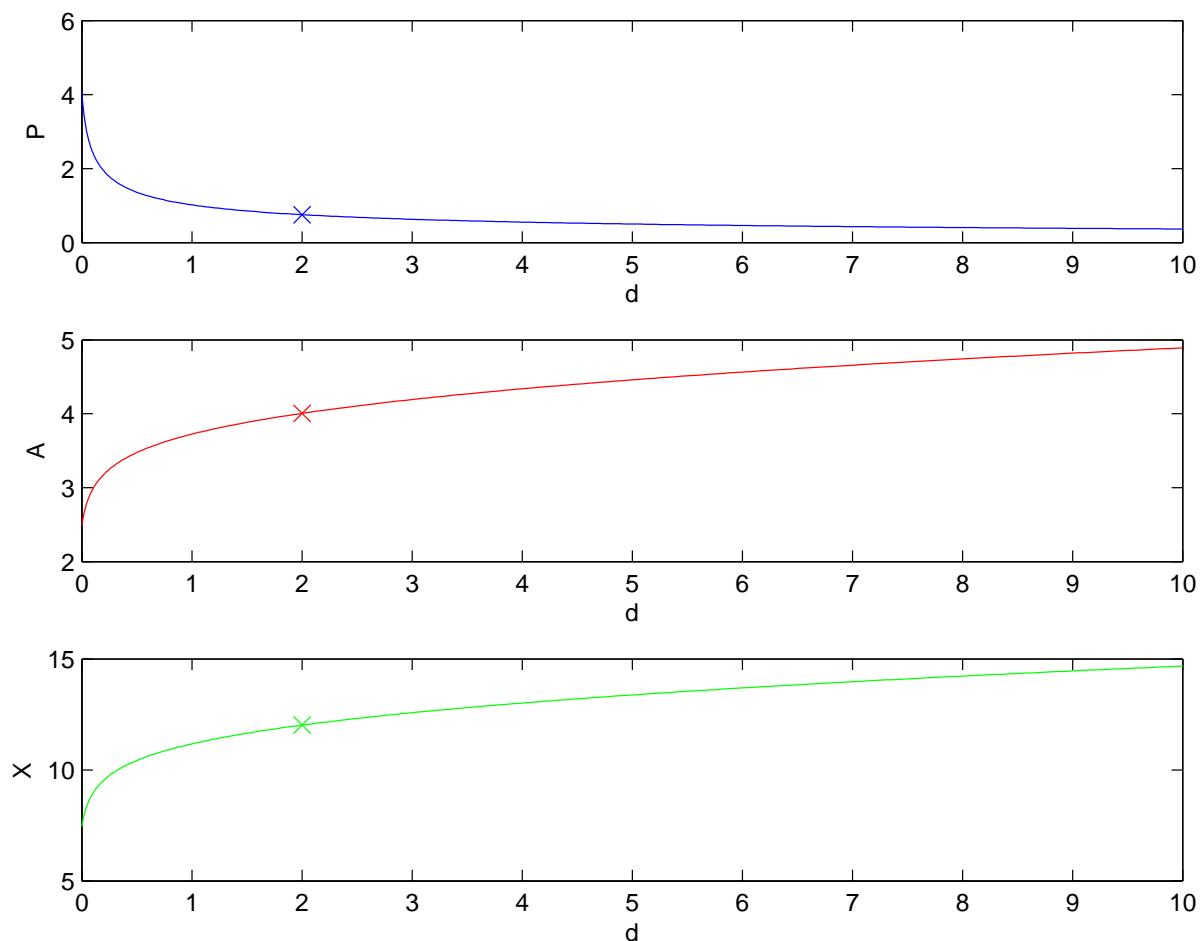


Figure 3.13: Bifurcation diagram for the parameter d : The upper panel displays the steady-state values for the pollution stock P , the middle one for the environmental absorption efficiency A and the lower one for the renewable natural resource X .

3.2.6 Parameter f - Carrying capacity of the renewable resource

The parameter f determines the carrying capacity of X , which is fA . Figure 3.14 displays the equilibrium values of the three state variables for varying f between 0 and 110. In the base case f is 10.

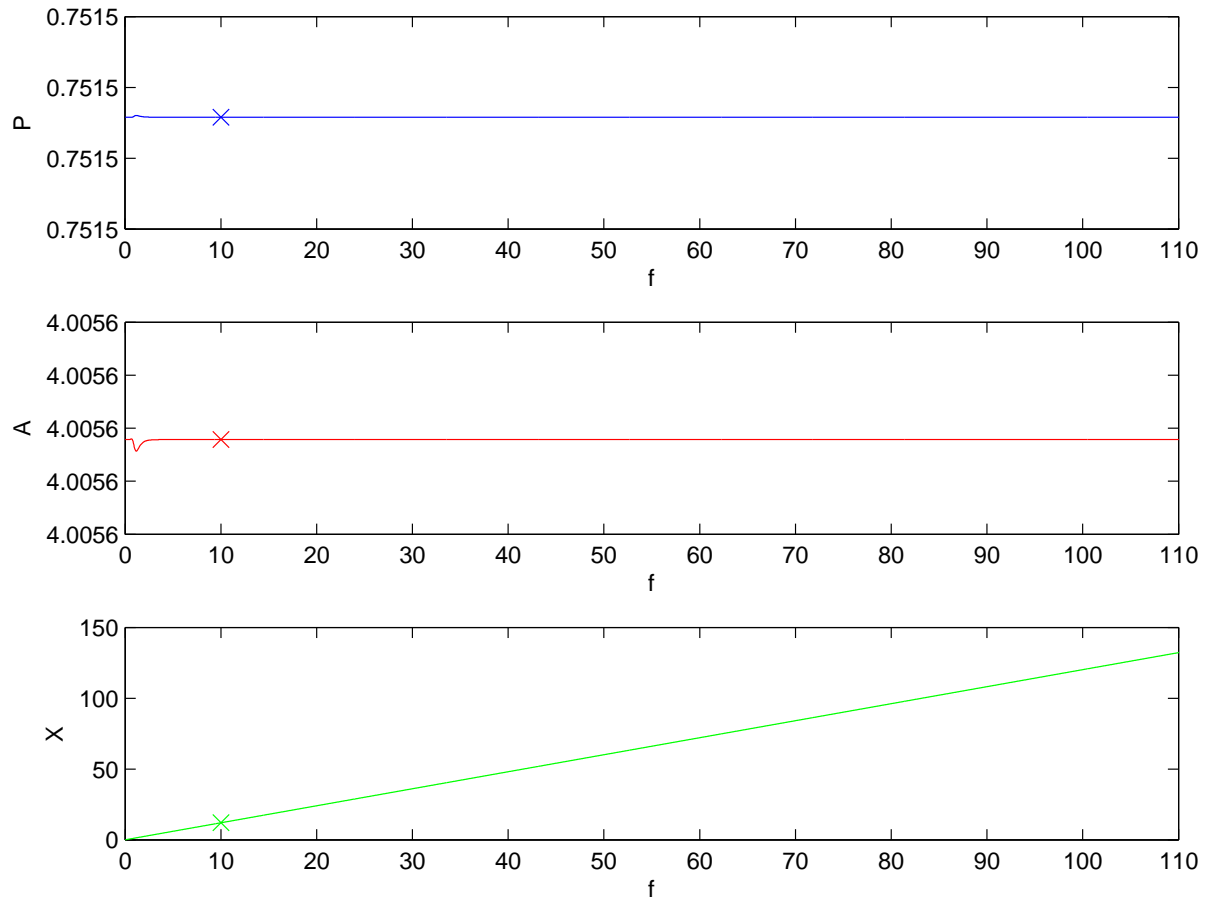


Figure 3.14: Bifurcation diagram for the parameter f : The upper panel displays the steady-state values for the pollution stock P , the middle one for the environmental absorption efficiency A and the lower one for the renewable natural resource X .

Changing the parameter f has no influence at all on the optimal long-run values of A and P . Only the value of X changes in that an increase in f results in a rise of the carrying capacity of the renewable natural resource and thus X increases.

One could also have expected that a change of the carrying capacity through f could be compensated by a change of A . But we have already seen that in most scenarios X is depending on A and not the other way round.

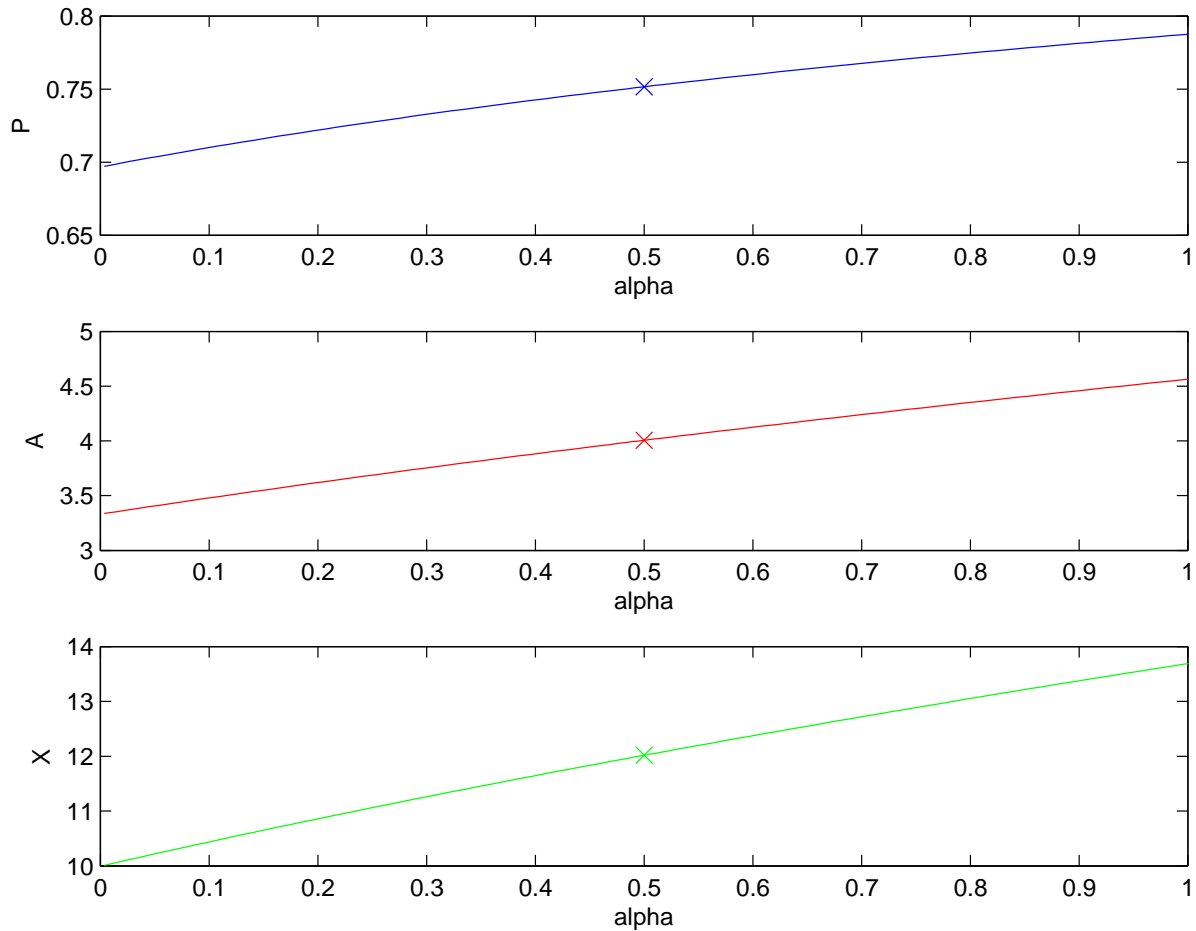


Figure 3.15: Bifurcation diagram for the parameter α : The upper panel displays the steady-state values for the pollution stock P , the middle one for the environmental absorption efficiency A and the lower one for the renewable natural resource X .

3.2.7 Parameter α - Direct effect of deforestation on the pollution

The parameter α determines the size of the impact of deforestation on the pollution stock. In Figure 3.15 we can see the bifurcation diagrams for α between zero and one. The base value of α is 0.5.

A higher value of α means that deforestation generates more pollution and so the equilibrium stock of pollution increases with increasing α . Moreover, rising α makes the destructive impact of deforestation higher compared to the one of production, and thus the optimal long-run level of production increases, while deforestation decreases a little. However, all this influences are rather little: P varies only between 0.7 and 0.8.

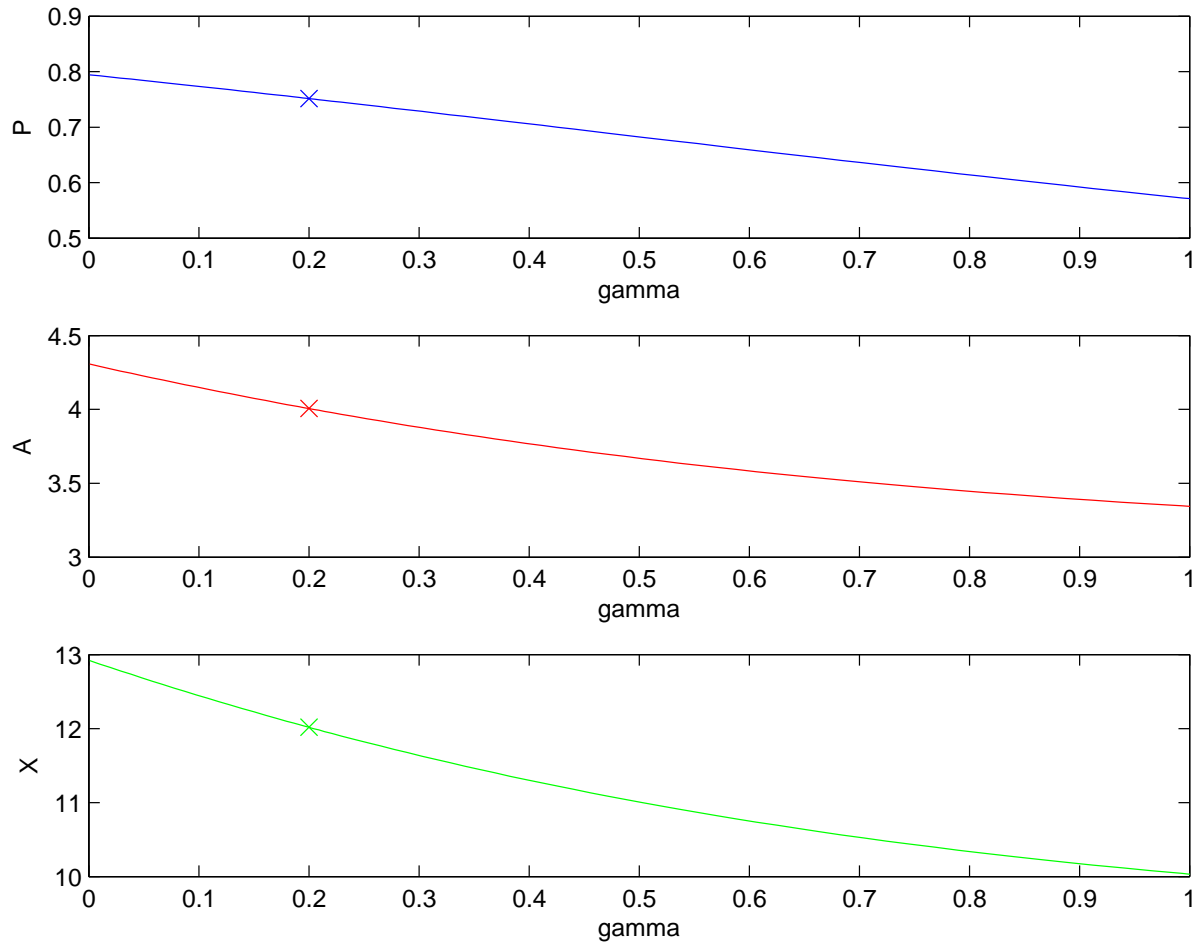


Figure 3.16: Bifurcation diagram for the parameter γ : The upper panel displays the steady-state values for the pollution stock P , the middle one for the environmental absorption efficiency A and the lower one for the renewable natural resource X .

3.2.8 Parameter γ - Influence of pollution on the absorption capacity

γ is the parameter measuring how big the destructive impact of the pollution stock is on the environmental absorption efficiency. The base value for γ is 0.2, and the bifurcation diagram in Figure 3.16 shows the optima for γ between zero and one.

With γ increasing, the steady-state values of A decrease not surprisingly. However, also the optimal long-run value of pollution P diminishes. That is because with higher γ the destructive impact of pollution would get too big if the stock of pollution were unchanged. Therefore the level of production is significantly reduced.

3.2.9 Summary

We have seen that almost all parameters have some significant effects on the steady states. Only the parameter f has no impact at all on the equilibrium levels of the pollution and the absorption capacity. An overview of the results derived in the sensitivity analysis is given in Table 3.3. Situations with multiple equilibria and indifference curves don't seem to occur in this model.

Parameter	P	A	X
r	↗	↘	↘
a	↗	↗	↗
b	↗	↘	↘
c	↘	↗	↗
d	↘	↗	↗
f	→	→	↗
α	↗	↗	↗
γ	↘	↘	↘

Table 3.3: Effects of changing a parameter value on the steady-state values of pollution P , environmental absorption efficiency A and renewable natural resource X .

The biggest changes in the optimal long-run value are triggered by changing the discount rate r . A striking result of this sensitivity analysis is also that the renewable natural resource X doesn't really have an influence on the other variables, except for f it only changes when the absorption capacity A varies and thus the bifurcation diagram of X is always of the same shape as the one for A .

3.3 Other Parameter Scenarios

In this section we will analyze the same optimal control model with different parameter settings and compare the results with the base case scenario described in Section 3.1. The parameters chosen are based upon the results of the sensitivity analysis. We have seen that the parameter r , the discount rate, has crucial influence on the outcome. Thus, we will investigate two situations where the discount rate is relatively low and high, respectively. Furthermore, we will consider a scenario where profits from deforestation are lower, i.e., the parameter b is lower than in the base case, and finally a situation where costs from pollution are estimated lower by setting the parameter d at a lower level. The results for all these scenarios are compared in Table B.1 in Appendix B.

3.3.1 High discount rate r

We start with analyzing the scenario where the social planner is quite myopic, i.e., the discount rate r is high. The bifurcation diagram for the parameter r in Figure 3.7 shows that the population of the renewable natural resource X converges to zero, when r goes to one. For r greater or equal to one no equilibrium point exists. For the analysis we set the discount rate $r = 0.9$ and let all the other parameters unchanged. The parameter setting is given in Table 3.4.

Model parameter	Parameter value
r	0.9
a	1
b	1
c	1
d	2
f	10
α	0.5
γ	0.2

Table 3.4: Parameter settings in Subsection 3.3.1.

State variables		Costate variables		Control variables	
P^*	0.96	λ_1^*	-0.84	e^*	1.19
A^*	1.62	λ_2^*	0.93	u^*	0.74
X^*	0.81	λ_3^*	1.30	v^*	0.95
				w^*	0.93

Table 3.5: Steady-state values in Subsection 3.3.1 where $r = 0.9$.

As already derived in Subsection 3.2.1, as a consequence of the myopic behavior, the steady-state value of pollution P is higher than in the base case, while the equilibrium levels of the environmental absorption capacity A and the renewable natural resource X are much lower than in the base case. The steady-state results are summarized in Table 3.5. The corresponding phase portrait can be seen in Figure 3.17. It looks similar to the one for the base case (cf. Figure 3.1). One difference which we can see is that in situations, where the population of X is almost zero in the beginning, it essentially doesn't start growing before not only the equilibrium level of P but also the one of A is almost reached.

Comparing the equilibrium values of the control variables in this scenario (Table 3.5) with the results in the base case (Table 3.2), we notice that the long-run deforestation rate u^* and especially the production rate e^* are lower than in the base case scenario.

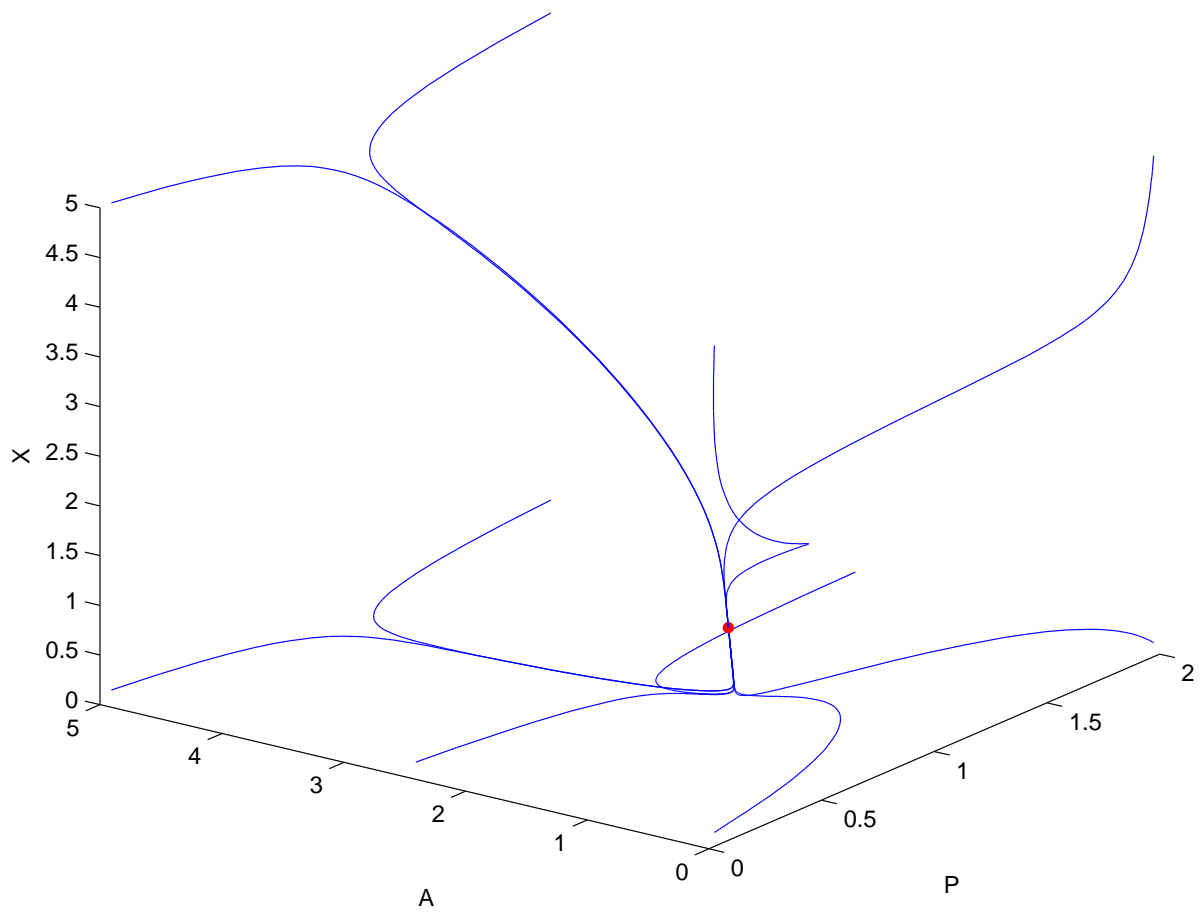


Figure 3.17: Phase portrait of the three state variables (pollution P , absorption capacity A , renewable natural resource X) for the scenario where $r = 0.9$.

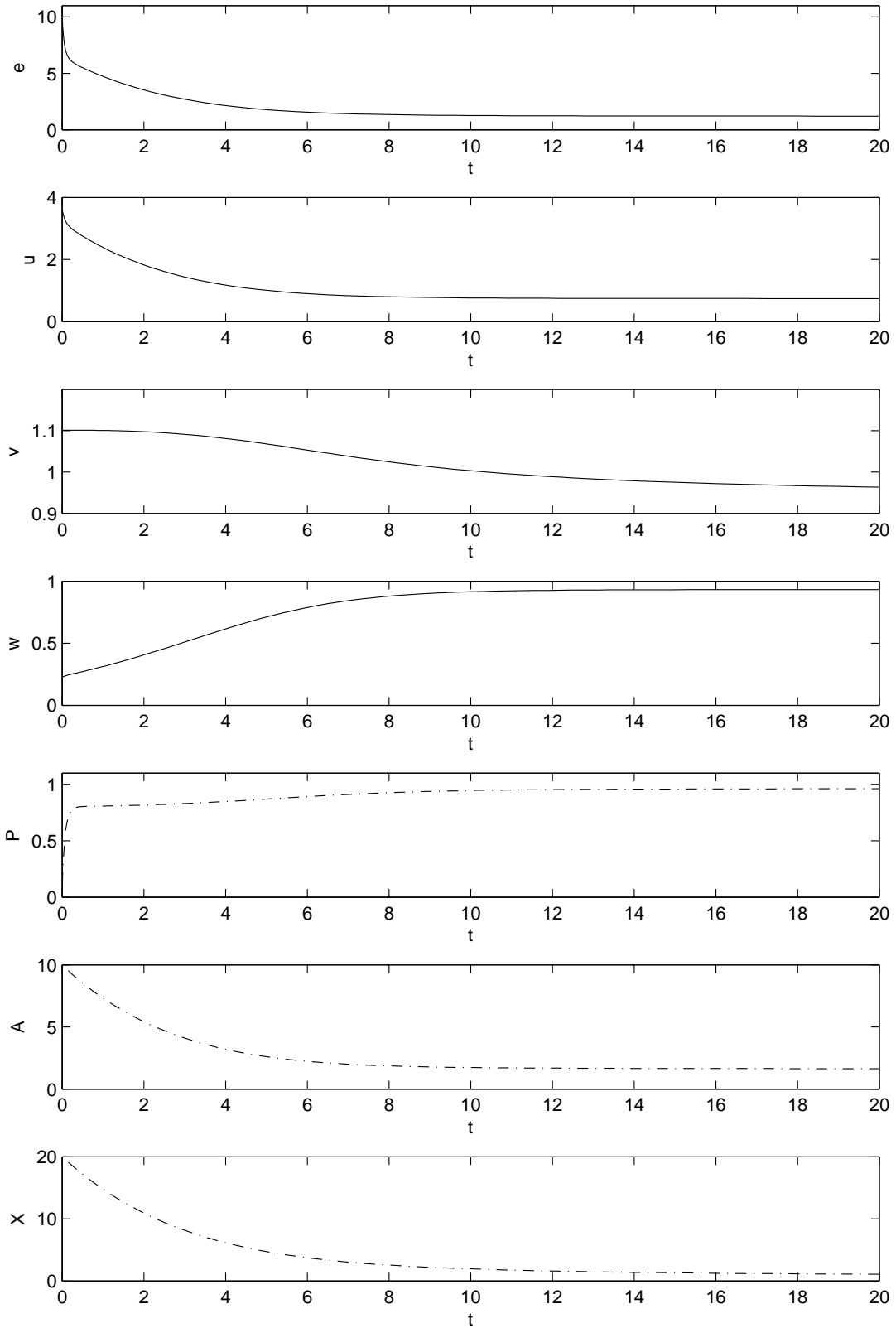


Figure 3.18: Time paths of the four control variables (production e , deforestation u , harvesting v , restoration w) and the three state variables (pollution P , absorption capacity A , renewable natural resource X) for the trajectory starting in $(0.05, 10, 20)$ when $r = 0.9$.

On the other hand, the harvesting rate v^* is higher, but this doesn't mean that the yield of harvesting is higher, since X^* is much lower. The restoration effort w^* is only slightly lower than in the base case. When the discount rate r is high, the revenues in the far future aren't considered that valuable and therefore are much lower. In return, revenues near to the present should be higher.

We want to analyze this by studying the time paths for the trajectory starting in a favorable initial situation, where pollution is almost zero and the absorption capacity and the stock of the renewable resource are high. The trajectory starting in $(0.05, 10, 20)$ is shown in Figure 3.18 and can be compared with the corresponding base case time paths in Figure 3.5.

The beginning of the dynamics of the production rate e , when $r = 0.9$, is similar to the base case: It doesn't start from a significantly higher level than in the base case, but is only half of the base-case production rate in the long run. So there are no additional revenues from production near to the present. As a consequence of the initially high production, in both scenarios the stock of pollution climbs immediately from 0 to around 0.75, but while P remains on this level in the base case, when $r = 0.9$ it still grows significantly until $t \approx 10$, reaching almost the level of 1. That is mainly because of too low support from the absorption capacity, which declines much faster than in the base case.

The shape of the dynamics of the control u is also similar in both scenarios, but in the beginning revenues from deforestation are much higher, while in the long run they are even a little bit lower than in base case. Moreover, there are some savings from lower restoration costs in the starting situation. On the downside, these differences in the beginning cause the environmental absorption capacity falling to levels lower than 2 at $t \approx 6$.

As expected, the dynamics of the renewable natural resource X are also different. When r is higher, the population isn't increasing in the beginning. Instead, it starts decreasing right in the beginning and doesn't stop until the resource is almost extinct. That is because v is much larger, and moreover the carrying capacity is lower because of lower absorption efficiency.

3.3.2 Low discount rate r

Now we want to analyze a situation where the discount rate r is lower, i.e., the social planner's decisions are rather future-oriented. For that purpose, we set the parameter $r = 0.1$ and let all the other model parameters unchanged. The parameter setting for the analysis in this subsection are summarized in Table 3.6.

Table 3.7 shows the steady-state values of the equilibrium for these parameters. As

Model parameter	Parameter value
r	0.1
a	1
b	1
c	1
d	2
f	10
α	0.5
γ	0.2

Table 3.6: Parameter settings in Subsection 3.3.2.

State variables		Costate variables		Control variables	
P^*	0.67	λ_1^*	-0.09	e^*	11.45
A^*	17.71	λ_2^*	1.05	u^*	0.91
X^*	79.68	λ_3^*	0.02	v^*	0.55
				w^*	1.05

Table 3.7: Steady-state values in Subsection 3.3.2 where $r = 0.1$.

we have already seen in the bifurcation diagrams in Figure 3.8, the equilibrium level of the environmental absorption capacity A and especially the one of the renewable natural resource X are much higher than in the base case scenario. The stock of pollution is only marginally lower in the equilibrium point. Moreover, we can see that a more future-oriented optimization leads to a more than four times higher production level in the long run, while the costs for restoration efforts are only slightly higher compared to the base case (cf. Table 3.2). The equilibrium harvesting rate v is significantly smaller, but since the population of the resource is much bigger, there is more long-run revenue from harvesting when $r = 0.1$.

A phase portrait for this parameter scenario is presented in Figure 3.19. There we can observe that in starting situations with an initial absorption capacity A higher than in the steady state and rather low starting population of the resource X , it is optimal to let X grow very fast to even higher levels than the equilibrium level in order to take advantage of an initially high carrying capacity.

Next we want to analyze the time paths for the trajectory starting in the point $(0.05, 10, 20)$, which is shown in Figure 3.20. At the beginning, the production rate e is quite high and decreases very quickly until the stock of pollution is close to its steady-state value. This is similar to the time paths we have seen for $r = 0.4$ and $r = 0.9$. However, while in those two cases e continues decreasing, here the production starts increasing again and even reaches a long-run production level four times higher than in

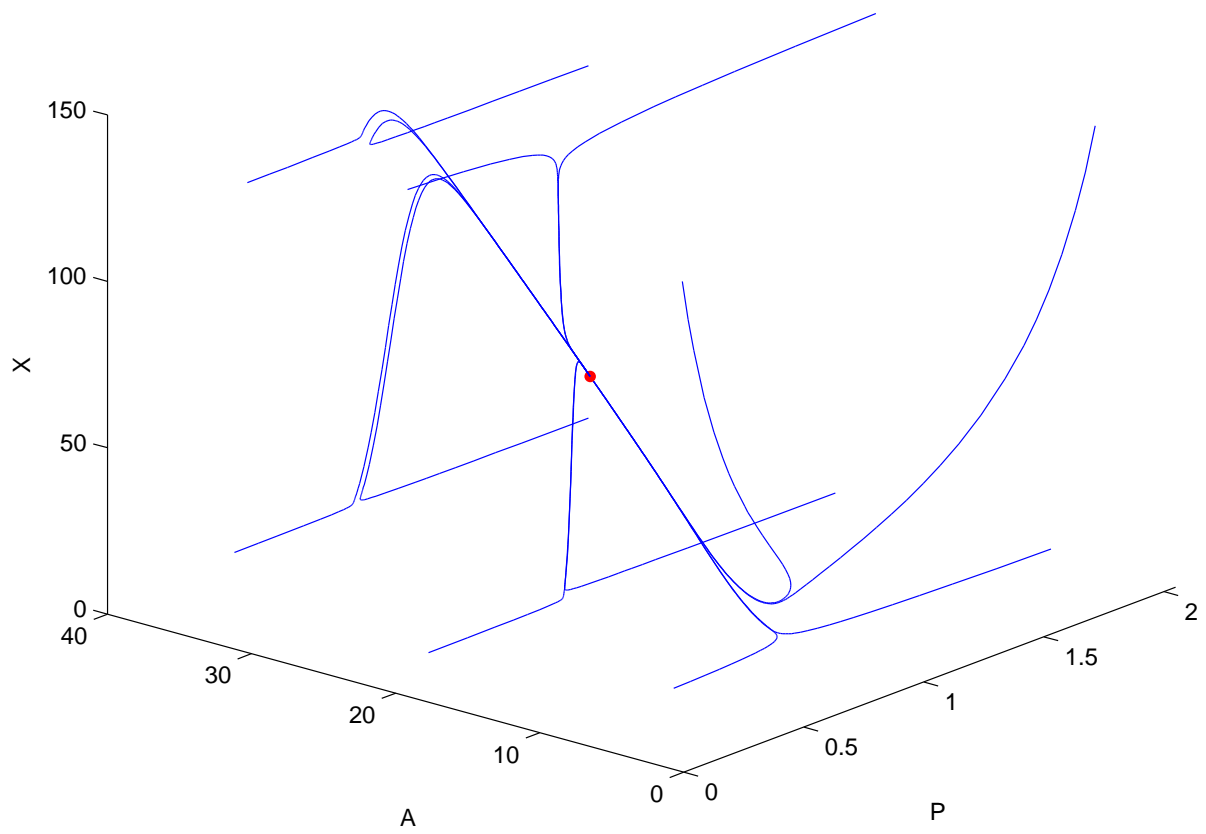


Figure 3.19: Phase portrait of the three state variables (pollution P , absorption capacity A , renewable natural resource X) for the scenario where $r = 0.1$.

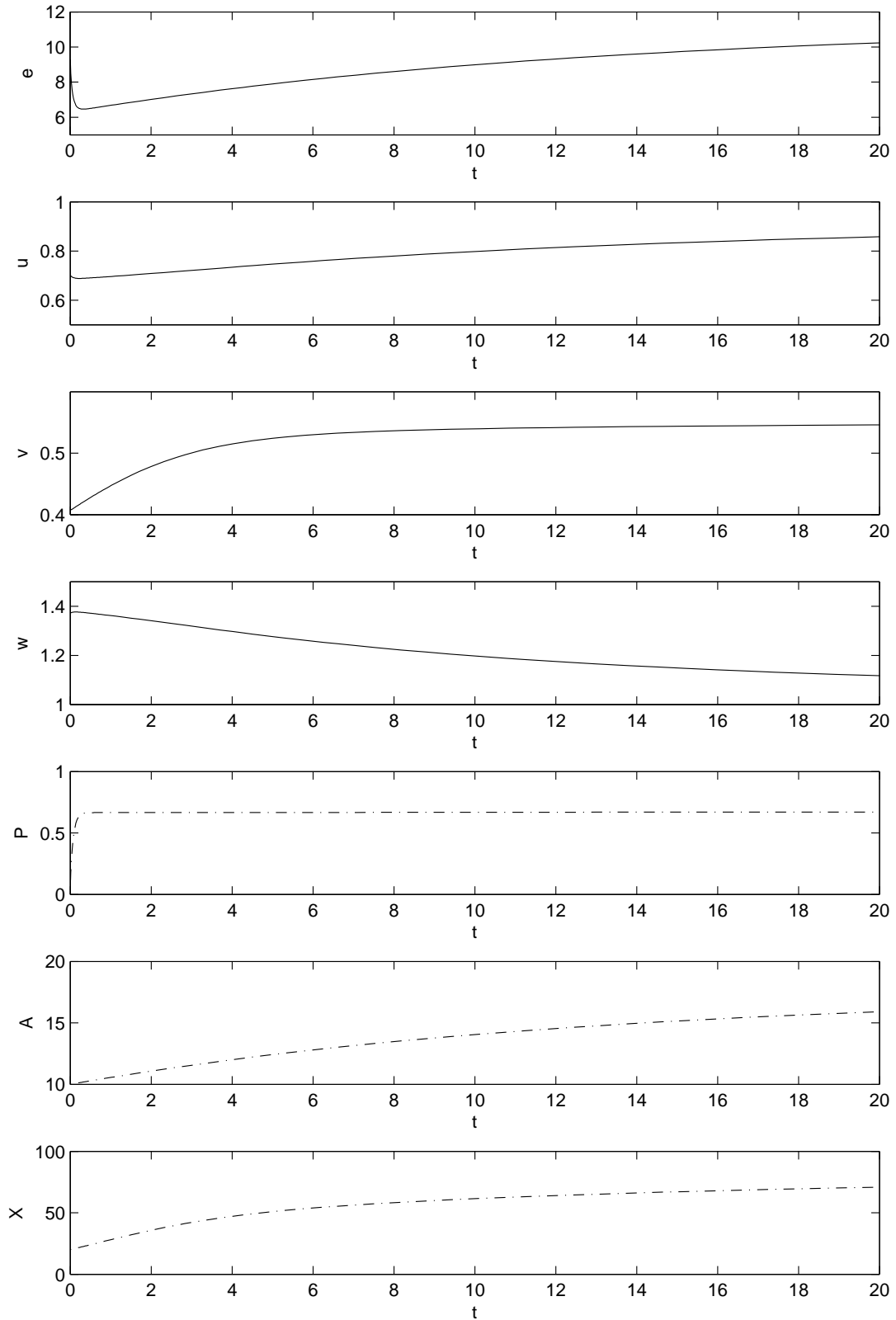


Figure 3.20: Time paths of the four control variables (production e , deforestation u , harvesting v , restoration w) and the three state variables (pollution P , absorption capacity A , renewable natural resource X) for the trajectory starting in $(0.05, 10, 20)$ when $r = 0.1$.

the base case scenario. The dynamics of the deforestation rate u are also different: For higher values of r it is initially higher and later decreases towards the equilibrium. When $r = 0.1$, it is the opposite, i.e. the control u is around 0.7 in the starting point and then increases slowly. The harvesting rate v is not only rather low in the steady state compared to a situation with a higher discount rate, in the beginning it is even a little bit lower, so that X increases although already starting at a high initial value. The restoration rate w is much higher in this scenario, particularly in the beginning there are significantly higher restoration costs, but in return the absorption efficiency A grows considerably and a sustainable high production level can be reached.

3.3.3 Lower profits from deforestation

In the sensitivity analysis we have seen that the system also reacts rather sensitively on the parameter b , particularly when b is getting low. Therefore we set the parameter $b = 0.05$ and analyze this new parameter scenario, implying an economy where deforestation isn't really profitable compared to harvesting and production. Revenues from these two economic activities are now supposed to be 20 times higher than revenues from deforestation. A situation like this could occur, for example, if there were almost no demand for wood of rainforests.

Model parameter	Parameter value
r	0.4
a	1
b	0.05
c	1
d	2
f	10
α	0.5
γ	0.2

Table 3.8: Parameter settings in Subsection 3.3.3.

State variables		Costate variables		Control variables	
P^*	0.71	λ_1^*	-0.11	e^*	8.78
A^*	12.52	λ_2^*	0.29	u^*	0.15
X^*	37.57	λ_3^*	0.04	v^*	0.70
				w^*	0.29

Table 3.9: Steady-state values in Subsection 3.3.3 where $b = 0.05$.

The model parameters for the analysis in this subsection are summarized in Table 3.8,

and the results for the steady state of this scenario are shown in Table 3.9. Looking at the equilibrium levels of the state variables and comparing them with the base case (cf. Table 3.2), we notice that the stock of pollution P is almost the same, while the absorption capacity A and thus also the renewable resource X are significantly higher. There is also far more production, but the deforestation rate is only approximately 0.15. Moreover, expenses for restoration are also less.

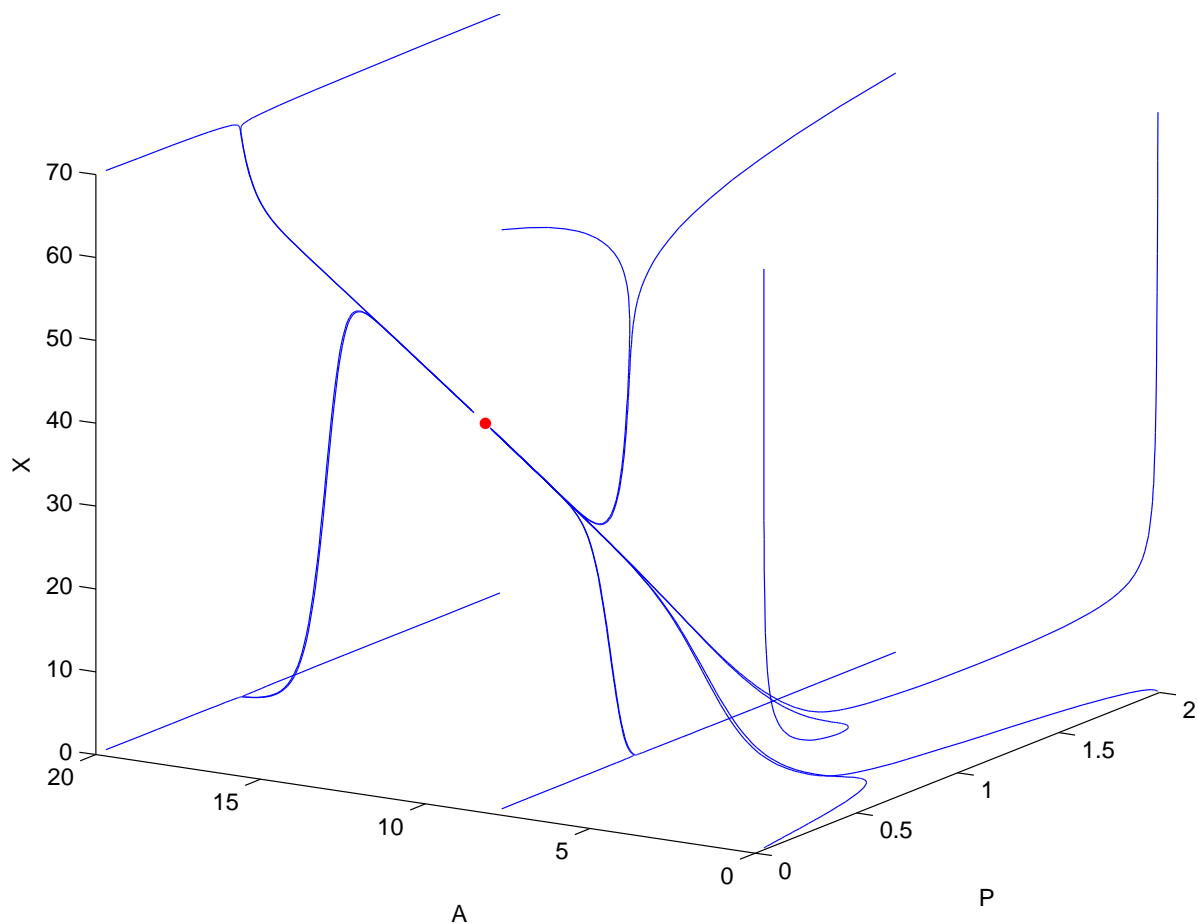


Figure 3.21: Phase portrait of the three state variables (pollution P , absorption capacity A , renewable natural resource X) for the scenario where $b = 0.05$.

The phase portrait of the three state variables presented in Figure 3.21 again isn't essentially qualitatively different from what we have already seen for other parameter settings. In particular it is similar to the phase portrait in Figure 3.19: X is initially increasing or decreasing rapidly depending on whether the absorption efficiency rate A is higher or lower than its equilibrium level, respectively.

In order to compare the time paths with the other parameter scenarios, we again consider them for the trajectory starting in the initial point $(0.05, 10, 20)$, which is presented in Figure 3.22. The main difference to the base case scenario, where A is diminishing

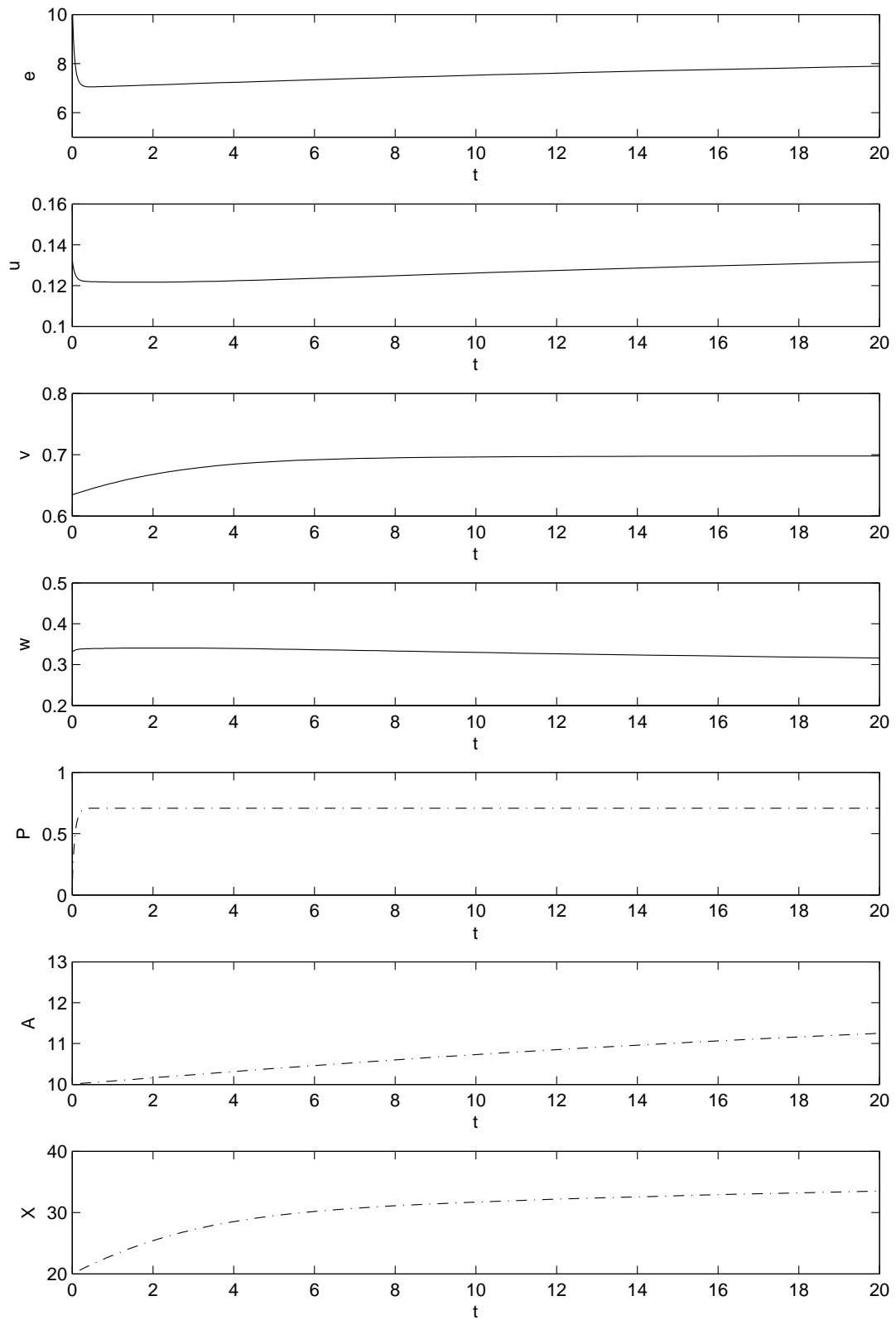


Figure 3.22: Time paths of the four control variables (production e , deforestation u , harvesting v , restoration w) and the three state variables (pollution P , absorption capacity A , renewable natural resource X) for the trajectory starting in $(0.05, 10, 20)$ when $b = 0.05$.

in the beginning, is that A is still continuously increasing, although its initial value is already rather high. As a consequence, the population of X is growing concavely and can reach a significantly higher equilibrium level. Moreover, because of the continuously improving support from the absorption capacity A , the production level e can increase slowly without having an increasing impact on the stock of pollution P . The restoration rate w isn't changing much over the time and is constantly low, mainly because there is much less deforestation. Furthermore, we can see that the dynamics of the state variables A and X and the control e towards their equilibrium levels are slower than in the parameter scenarios we have seen so far, where at $t = 20$ all the variables have already almost reached their steady-state values.

3.3.4 Lower costs of pollution

In the base case scenario we assume $d = 2$. Now we want to analyse in detail a situation with the assumption of lower costs from pollution. Therefore we set $d = 0.5$. The values of all the model parameters can be seen in Table 3.10. The sensitivity with respect to this parameter is also of special interest because it is not really easy to quantify and estimate the costs from pollution.

Model parameter	Parameter value
r	0.4
a	1
b	1
c	1
d	0.5
f	10
α	0.5
γ	0.2

Table 3.10: Parameter settings in Subsection 3.3.4.

State variables		Costate variables		Control variables	
P^*	1.36	λ_1^*	-0.23	e^*	4.31
A^*	3.48	λ_2^*	1.10	u^*	0.82
X^*	10.42	λ_3^*	0.14	v^*	0.70
				w^*	1.10

Table 3.11: Steady-state values in Subsection 3.3.4 where $d = 0.5$.

The phase portrait presented in Figure 3.23 looks again fairly similar to the phase portrait for the base case (cf. Figure 3.1), except for the fact that the equilibrium point

is different. The steady-state values are given in Table 3.11. The stock of pollution is almost double as high as in the base case, where $d = 2$, while the absorption efficiency is only slightly lower in the equilibrium. The long-run production rate is much higher and also the restoration rate is a little bit higher. Deforestation is nearly the same as in the base case.

The time paths for the trajectory starting in $(0.05, 10, 20)$ are shown in Figure 3.24. The shapes of the curves for all the state and control variables are basically the same as in the base case scenario (cf. Figure 3.5), but the production level e is much higher than in the base case and is also decreasing less. As a consequence, pollution P is also increasing to a higher level in the beginning. But after growing initially from 0 to approximately 1.36, the stock of pollution isn't changing any more like in the base case.

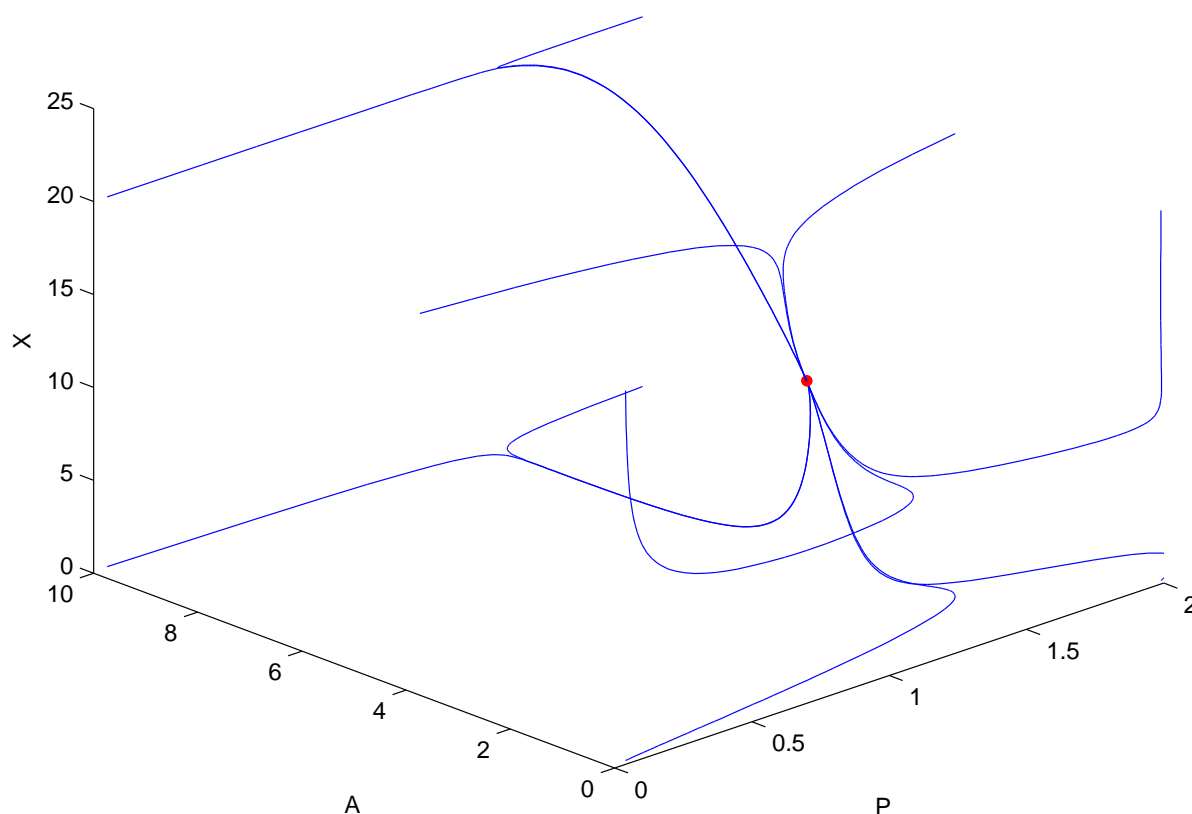


Figure 3.23: Phase portrait of the three state variables (pollution P , absorption capacity A , renewable natural resource X) for the scenario where $d = 0.5$.

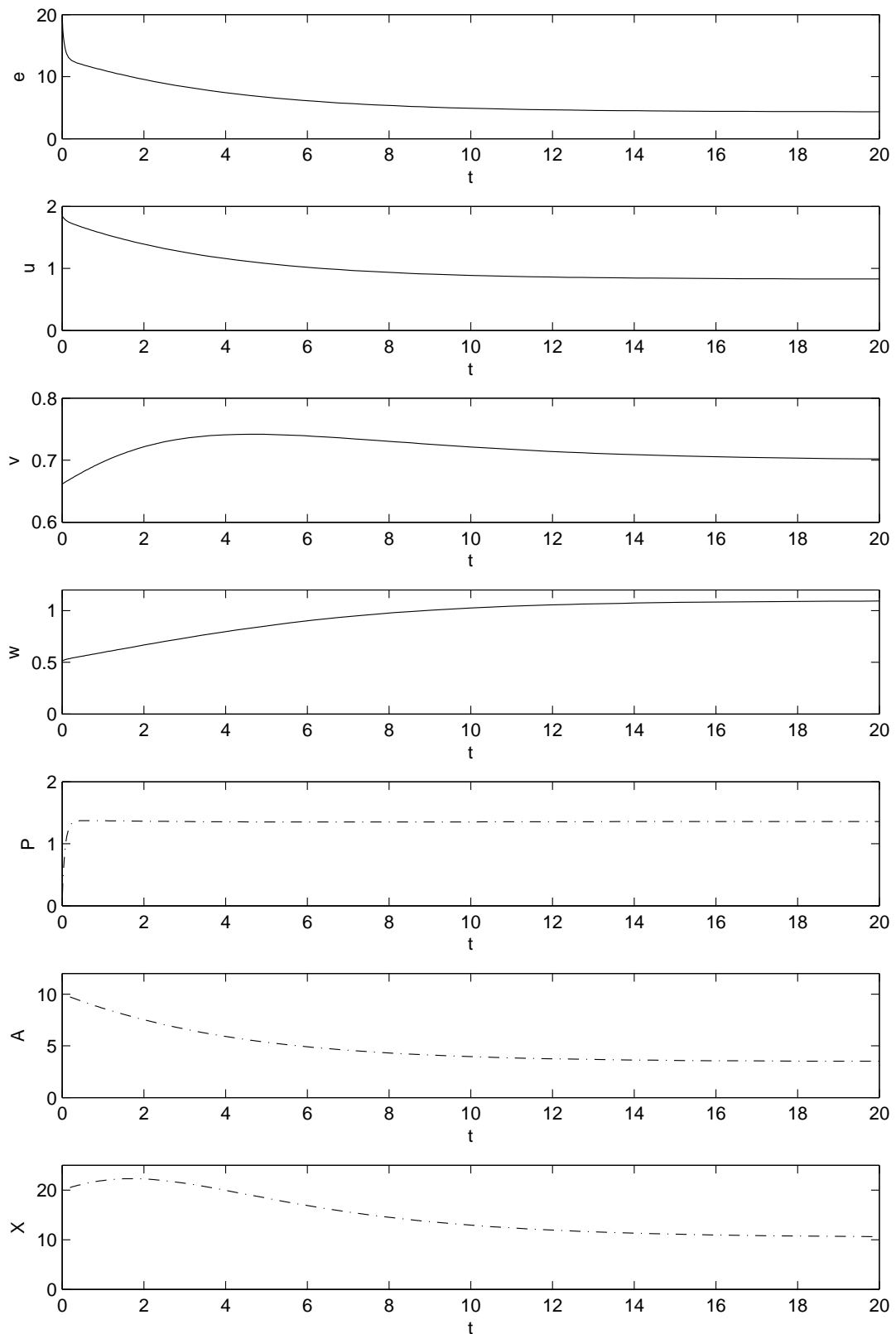


Figure 3.24: Time paths of the four control variables (production e , deforestation u , harvesting v , restoration w) and the three state variables (pollution P , absorption capacity A , renewable natural resource X) for the trajectory starting in $(0.05, 10, 20)$ when $d = 0.5$.

Chapter 4

Summary and Conclusions

In this Master's thesis an autonomous infinite horizon optimal control model was defined. It consists of the three state variables pollution P , environmental absorption efficiency A and renewable natural resource X as well as the four control variables production e , deforestation u , harvesting v and restoration w . The necessary optimality conditions provided by the maximum principle lead to a six-dimensional canonical system, which can be reduced to a three-dimensional system but cannot be completely solved analytically. From the analytical analysis we can see that the steady state of the resource X depends only linearly on the steady-state value of A . Moreover, we notice that for $r \geq 1$ no steady state exists because of the condition $X > 0$.

The numerical analysis is carried out with the help of the MATLAB toolbox OCMat. The result of the search for equilibrium points is a single steady state with $P^* = 0.75$, $A^* = 4.01$ and $X^* = 12.02$ in the base case scenario. The phase portrait of the three state variables shows that the pollution stock is changing its level extremely fast towards its steady-state value and isn't changing significantly after the beginning. Time paths of trajectories starting in initial states, where P and A are starting from the same level and only X is different, show that the dynamics of the renewable resource X don't have influence from other state or control variables besides the harvesting rate v .

The sensitivity analysis reveals that the solution of the model is much sensitive when parameter values of r , b and d change, especially when they are getting small and converging to zero. Besides the case where $r \geq 1$, for all the parameters values considered, always one single equilibrium point exists in the admissible range. There is no situation where a bifurcation occurs and thus we have no multiple equilibria and indifference curves, phenomena which often occur in optimal control models. Furthermore, it is also remarkable that except for the parameters r and f all bifurcation diagrams are qualitatively of the same shape. This is not surprising and can be seen from Equation (2.29), since X linearly depends on A as already mentioned. The signs of the effects of changing

a model parameter are also as expected; an overview is given in Table 3.3.

In Section 3.3 some other parameter scenarios are analyzed in detail. Basically the structure of the solutions doesn't vary much as the phase portraits show, while the values of the equilibrium points differ significantly. An overview of these results is provided in table B.1.

The discount rate r apparently has a crucial influence on the long-run levels of the system. The results of this model suggest that a future-oriented behavior can lead to a significantly more desirable equilibrium. This doesn't only mean a better state of the environment (i.e., a lower stock of pollution and a higher environmental absorption efficiency), but also enables a much higher level of production in the long run. Furthermore, the initially lower utilities compared to a myopic solution with a high discount rate are comparatively small: Mostly there are more revenues from deforestation and lower costs for restoration in the beginning, the production level doesn't vary much initially.

Also interesting are the results from the scenario, where almost no gains from deforestation can be made. It is not surprising that this implies of course to a shift to the production sector. In the steady state, the emissions from production are more than three times higher than in the base case. Nevertheless, the stock of pollutions is only slightly higher because there is much more absorption capacity in the long run due to less deforestation.

The improvement of the better state of the environment for the scenario with low discount rate mainly consists of higher environmental absorption efficiency. The equilibrium stock of pollution doesn't change that much in all these situations. So the model in this thesis implies a crucial importance of oceans and land as CO₂ sinks.

Appendix A

Optimal Control Theory

The optimal control model defined in this thesis belongs to the class of autonomous infinite horizon problems, which are generally of the following form:

$$\begin{aligned} & \max_{u(\cdot)} \int_0^{\infty} e^{-rt} g(x(t), u(t)) dt \\ & \text{s.t. } \dot{x}(t) = f(x(t), u(t)), t \geq 0 \\ & \text{with } x(0) = x_0, \end{aligned} \tag{A.1}$$

where $x(t) \in \mathbb{R}^n$ denotes the n state variables and $u(t) \in \mathbb{R}^m$ the m control variables of the optimal control model at time t . It is assumed that the integral converges for all admissible $(x(\cdot), u(\cdot))$. The objective function $g : \mathbb{R}^{n+m} \rightarrow \mathbb{R}$ and the state dynamics $f : \mathbb{R}^{n+m} \rightarrow \mathbb{R}^n$ are assumed to be continuously differentiable.

A dynamic optimization problem of this type can be solved with the application of Pontryagin's maximum principle. For that purpose, we need the current-value Hamiltonian function $H(x(\cdot), u(\cdot), \lambda(\cdot))$, which is defined by

$$H(x(t), u(t), \lambda(t), \lambda_0) = \lambda_0 g(x(t), u(t)) + \lambda(t) f(x(t), u(t)),$$

where $\lambda(t) \in \mathbb{R}^n$ are the costate variables, which can economically be interpreted as shadow prices.

The maximum principle delivers necessary optimality conditions. For this type of problem they are formulated as follows (cf. Grass et al. [2008]):

Let $(x^*(\cdot), u^*(\cdot))$ be an optimal solution of problem (A.1), then there exists a continuous and piecewise continuously differentiable function $\lambda(\cdot)$ and a constant $\lambda_0 \geq 0$

satisfying for all $t \geq 0$

$$\begin{aligned}(\lambda_0, \lambda(t)) &\neq 0 \\ H(x^*(t), u^*(t), \lambda^*(t), \lambda_0) &= \max_u H(x(t), u, \lambda(t), \lambda_0),\end{aligned}$$

and moreover at every point where $u(\cdot)$ is continuous the adjoint equation

$$\dot{\lambda}(t) = r\lambda(t) - H_x(x^*(t), u^*(t), \lambda(t), \lambda_0)$$

is satisfied.

Let $u^*(\cdot)$ be an admissible control to the problem (A.1) maximizing the Hamiltonian function, i.e., satisfying

$$u^*(t) \in \arg \max_u H(x(t), u, \lambda(t), \lambda_0),$$

then the differential equation system

$$\begin{aligned}\dot{x} &= f(x(t), u^*(t)) \\ \dot{\lambda} &= r\lambda(t) - H_x(x(t), u^*(t), \lambda(t))\end{aligned}$$

is called the canonical system of the optimal control model (A.1).

Appendix B

Overview of Results

	State variables			Control variables			
	P^*	A^*	X^*	e^*	u^*	v^*	w^*
Base Case	0.75	4.01	12.02	2.59	0.84	0.70	0.99
$r = 0.9$	0.96	1.62	0.81	1.19	0.74	0.95	0.93
$r = 0.1$	0.67	17.71	79.68	11.45	0.91	0.55	1.05
$b = 0.05$	0.71	12.52	37.57	8.78	0.15	0.70	0.29
$d = 0.5$	1.36	3.48	10.42	4.31	0.82	0.70	1.10

Table B.1: Comparison of the steady-state values for the base case scenario and the scenarios discussed in Section 3.3.

List of Tables

3.1	Parameter settings for the base case	21
3.2	Steady state values in the base case	28
3.3	Summary Sensitivity Analysis	51
3.4	Parameter settings in Subsection 3.3.1.	52
3.5	Steady-state values in Subsection 3.3.1 where $r = 0.9$	52
3.6	Parameter settings in Subsection 3.3.2.	56
3.7	Steady-state values in Subsection 3.3.2 where $r = 0.1$	56
3.8	Parameter settings in Subsection 3.3.3.	59
3.9	Steady-state values in Subsection 3.3.3 where $b = 0.05$	59
3.10	Parameter settings in Subsection 3.3.4.	62
3.11	Steady-state values in Subsection 3.3.4 where $d = 0.5$	62
B.1	Comparison of the steady-state values for the base case scenario and the scenarios discussed in Section 3.3.	69

List of Figures

3.1	Phase portrait for the base case	30
3.2	Time paths for trajectory 1	34
3.3	Time paths for trajectory 2	35
3.4	Time paths for trajectory 3	37
3.5	Time paths for trajectory 4	38
3.6	Time paths for trajectory 5	39
3.7	Bifurcation diagram for the parameter r	41
3.8	Bifurcation diagram for small r	42
3.9	Bifurcation diagram for the parameter a	43
3.10	Bifurcation diagram for the parameter b	44
3.11	Bifurcation diagram for small b	45
3.12	Bifurcation diagram for the parameter c	46
3.13	Bifurcation diagram for the parameter d	47
3.14	Bifurcation diagram for the parameter f	48
3.15	Bifurcation diagram for the parameter α	49
3.16	Bifurcation diagram for the parameter γ	50
3.17	Phase portrait ($r = 0.9$)	53
3.18	Time paths for trajectory 4 ($r = 0.9$)	54
3.19	Phase portrait ($r = 0.1$)	57
3.20	Time paths for trajectory 10 ($r = 0.1$)	58
3.21	Phase portrait ($b = 0.05$)	60
3.22	Time paths for trajectory 13 ($b = 0.05$)	61
3.23	Phase portrait ($d = 0.5$)	63
3.24	Time paths for trajectory 4 ($d = 0.5$)	64

Bibliography

- A. D. Ayong Le Kama. Sustainable growth, renewable resources and pollution. *Journal of Economic Dynamics and Control*, 25(12):1911–1918, 2001.
- A. Beltratti, G. Chichilnisky, and G. M. Heal. Sustainable growth and the green golden rule. In I. Goldin and L. A. Winters, editors, *The Economics of Sustainable Development*. Cambridge University Press, Cambridge, 1994.
- J. G. Canadell, C. Le Quéré, M. R. Raupach, C. B. Field, E. T. Buitenhuis, P. Ciais, T. J. Conway, N. P. Gillett, R. A. Houghton, and G. Marland. Contributions to accelerating atmospheric CO₂ growth from economic activity, carbon intensity, and efficiency of natural sinks. *Proceedings of the National Academy of Sciences*, 104(47):18866–18870, 2007.
- A. Dhooge, W. Govaerts, Yu. A. Kuznetsov, W. Mestrom, A. M. Riet, and B. Sautois. *MATCONT and CL MATCONT: Continuation Toolboxes in Matlab*, 2006. URL <http://www.matcont.ugent.be/manual.pdf>. Accessed on April 16, 2015.
- E. Dlugokencky and P. Tans. Trends in atmospheric carbon dioxide (NOAA/ESRL). <http://www.esrl.noaa.gov/gmd/ccgg/trends/global.html>, 2015. Accessed on May 4, 2015.
- F. El Ouardighi. Emissions, deforestation and renewable resource harvesting under time-dependent environmental absorption efficiency. Mimeo, 2015.
- F. El Ouardighi, H. Benchekroun, and D. Grass. Controlling pollution and environmental absorption capacity. *Annals of Operations Research*, 220:111–133, 2014.
- D. Grass. Numerical computation of the optimal vector field: Exemplified by a fishery model. *Journal of Economic Dynamics and Control*, 36(10):1626–1658, 2012.
- D. Grass and A. Seidl. *OCMat v0.1 Manual*, 2014. URL http://orcos.tuwien.ac.at/fileadmin/t/orcos/OCMat/ocmat_manual_01.pdf. Accessed on October 4, 2014.

- D. Grass, J. P. Caulkins, G. Feichtinger, G. Tragler, and D. A. Behrens. *Optimal Control of Nonlinear Processes: With Applications in Drugs, Corruption, and Terror*. Springer Verlag, Berlin, 2008.
- IPCC. *Climate Change 2013: The Physical Science Basis. Contribution of Working Group I to the Fifth Assessment Report of the Intergovernmental Panel on Climate Change*. Cambridge University Press, 2013.
- C. Le Quéré, R. Moriarty, R. M. Andrew, G. P. Peters, P. Ciais, P. Friedlingstein, S. D. Jones, S. Sitch, P. Tans, A. Arneeth, T. A. Boden, L. Bopp, Y. Bozec, J. G. Canadell, F. Chevallier, C. E. Cosca, I. Harris, M. Hoppema, R. A. Houghton, J. I. House, A. Jain, T. Johannessen, E. Kato, R. F. Keeling, V. Kitidis, K. Klein Goldewijk, C. Koven, C. S. Landa, P. Landschützer, A. Lenton, I. D. Lima, G. Marland, J. T. Mathis, N. Metzl, Y. Nojiri, A. Olsen, T. Ono, W. Peters, B. Pfeil, B. Poulter, M. R. Raupach, P. Regnier, C. Rödenbeck, S. Saito, J. E. Salisbury, U. Schuster, J. Schwinger, R. Séférian, J. Segschneider, T. Steinhoff, B. D. Stocker, A. J. Sutton, T. Takahashi, B. Tilbrook, G. R. van der Werf, N. Viovy, Y.-P. Wang, R. Wanninkhof, A. Wiltshire, and N. Zeng. Global carbon budget 2014. *Earth System Science Data Discussions*, 7 (2):521–610, 2014.
- O. Tahvonen. On the dynamics of renewable resource harvesting and pollution control. *Environmental and Resource Economics*, 1(1):97–117, 1991.